Title

Reorganization in the macaque interoceptive-allostatic network following anterior cingulate cortex damage

Journal

Cerebral Cortex, 33(8)

ISSN

1047-3211

Authors

Charbonneau, Joey A

Bennett, Jeffrey L

Chau, Kevin

et al.

Publication Date

2023-04-04

DOI

10.1093/cercor/bhac346

Peer reviewed

OXFORD

Cerebral Cortex, 2023, **33**, 4334–4349
https://doi.org/10.1093/cercor/bhac346
Advance access publication date 6 September 2022
Original Article

Reorganization in the macaque interoceptive-allostatic network following anterior cingulate cortex damage

Joey A. Charbonneau[1,2,*], Jeffrey L. Bennett[2,3,4], Kevin Chau[2], Eliza Bliss-Moreau[2,5,*]

[1]Neuroscience Graduate Program, University of California Davis, 1544 Newton Court, Davis, CA 95618, United States,
[2]California National Primate Research Center, University of California Davis, One Shields Avenue, Davis, CA 95616, United States,
[3]Department of Psychiatry and Behavioral Sciences, University of California Davis School of Medicine, 2230 Stockton Blvd, Sacramento, CA 95817, United States,
[4]The MIND Institute, University of California Davis, 2825 50th Street, Sacramento, CA 95817, United States,
[5]Department of Psychology, University of California Davis, 135 Young Hall One Shields Avenue, Davis, CA 95616, United States

*Corresponding authors: Neuroscience Graduate Program, University of California, Davis, One Shields Avenue, Davis, CA 95616, United States.
Email: jcharbonneau@ucdavis.edu; Department of Psychology, University of California Davis, One Shields Ave 95616. Email: eblissmoreau@ucdavis.edu

Accumulating evidence indicates that the adult brain is capable of significant structural change following damage—a capacity once thought to be largely limited to developing brains. To date, most existing research on adult plasticity has focused on how exteroceptive sensorimotor networks compensate for damage to preserve function. Interoceptive networks—those that represent and process sensory information about the body's internal state—are now recognized to be critical for a wide range of physiological and psychological functions from basic energy regulation to maintaining a sense of self, but the extent to which these networks remain plastic in adulthood has not been established. In this report, we used detailed histological analyses to pinpoint precise changes to gray matter volume in the interoceptive-allostatic network in adult rhesus monkeys (*Macaca mulatta*) who received neurotoxic lesions of the anterior cingulate cortex (ACC) and neurologically intact control monkeys. Relative to controls, monkeys with ACC lesions had significant and selective unilateral expansion of the ventral anterior insula and significant relative bilateral expansion of the lateral nucleus of the amygdala. This work demonstrates the capacity for neuroplasticity in the interoceptive-allostatic network which, given that changes included expansion rather than atrophy, is likely to represent an adaptive response following damage.

Key words: amygdala; brain damage; insula; plasticity; rhesus monkey.

Introduction

Although the neonatal brain's capacity for reorganization following damage has long been recognized (see Kolb and Gibb 2007 for a review), the extent to which the adult brain remains plastic following significant insult is still largely unknown. Work in animal models consistently demonstrates that damaging specific neural targets in the neonatal brain has less of a deleterious functional impact than damaging the same targets in the adult brain (as in the Kennard Principle; Kennard 1936, 1942). For example, damage to motor cortex in infant monkeys results in almost complete recovery of motor function, whereas similar damage in adulthood results in severe and lasting paresis (Kennard 1942). Such dissociations between brain damage that occurs early versus late in life are not restricted to sensorimotor regions, and have also been demonstrated in prefrontal cortex (e.g. Akert et al. 1960; Bachevalier et al. 2011) and subcortical structures like the amgydala (e.g. Mason et al. 2006; Bliss-Moreau et al. 2011, 2013; Kazama et al. 2012; Moadab et al. 2015) and the hippocampus (e.g. Banta Lavenex et al. 2006; Lavenex and Lavenex 2006), with critical periods for plasticity identified in infancy (Kolb 1989; O'Leary et al. 1994; Kolb and Gibb 2010). Although infancy appears to be the period in which the most significant neural plasticity can and does occur (Ismail et al. 2017; Kolb et al. 2017), there is growing recognition that the adult brain—once thought to be fairly static and incapable of large structural changes—also has a remarkable ability to compensate for damage, including both microstructural and macrostructural changes (Burke and Barnes 2006; Hübener and Bonhoeffer 2014; Power and Schlaggar 2017).

There is a long tradition in behavioral neuroscience of removing or modifying select regions of the nonhuman primate brain to understand their function (for a review see Vaidya et al. 2019). Despite a fairly large literature on functional effects of such lesions, there is very little research investigating how adult brains adapt to such damage (although see: Croxson et al. 2012; Murata et al. 2015; Chareyron et al. 2016; Froudist-Walsh et al. 2018). Studies of the macaque brain that explicitly investigate plasticity following discrete lesions have demonstrated that changes occur primarily in neuroanatomical regions to which damaged structures are connected (Crossley et al. 2014; Froudist-Walsh et al. 2018). The severity of functional deficits produced by discrete damage to the macaque brain also is dependent on the availability of neurotransmitters in connected regions (e.g. acetylcholine availability in inferotemporal cortex following fornix lesions; Croxson et al. 2012), further highlighting the importance of considering the impacts of discrete lesions within functional networks. Brain damage can result in a variety of different types of changes (e.g. diaschisis, degeneration, compensation, and degeneracy) and such changes may be either adaptive or maladaptive (see Fornito et al. 2015 for a review). Evidence from human patients who sustain major brain damage—typically caused by stroke (e.g. Rossini and Dal Forno 2004; Murphy and Corbett 2009) or surgical resections for the treatment of epilepsy or other neurological

Received: June 8, 2022. **Revised:** August 8, 2022. **Accepted:** August 9, 2022

disorders (e.g. Yogarajah et al. 2010; Sidhu et al. 2016)—shows that over time and via interventions (e.g. physical and occupational therapies: Behrman et al. 2006; neurorestorative therapies: Hermann and Chopp 2012; cognitive therapies: Lubrini et al. 2018), people are able to recover significant function (Robertson and Murre 1999; Turkeltaub 2019). Although powerful demonstrations of neural plasticity, such recovery trajectories in humans offer limited, if any, insight into the specific neural substrates that undergo plastic changes and also reflect heterogeneous insults to the brain, which makes drawing conclusions about specific brain regions and their plastic potential difficult. Evaluating structural plasticity in the brains of adult animals who sustained focal damage to specific neural hubs is therefore an important opportunity to understand plasticity mechanisms in adulthood.

The ability of the nervous system to respond to stimuli by reorganizing both structure and function, "neuroplasticity" (Jellinger and Attems 2013), can be revealed by many different levels of analysis (see Kolb and Gibb 2007, 2014; Sharma et al. 2013 for reviews). At a cellular level, where plastic changes are most often investigated, alterations occur to the intrinsic properties of cell membranes (Straka et al. 2005; Beck and Yaari 2008), morphology of dendrites and axons (Matus 2000; Gomis-Rüth et al. 2008), and the number or strength of synaptic contacts between cells (Turrigiano 2012; Vitureira et al. 2012), among other changes (see Abbott and Nelson 2000; Gulyaeva 2017 for reviews). Although it is assumed that micro-scale changes to cells and molecules ultimately lead to structure and system changes (Morrison and Baxter 2012; Stee and Peigneux 2021), changes at the level of structures are likely to be most relevant for translational science (e.g. diagnostics in humans, typically using magnetic resonance imaging, MRI; Fossati et al. 2004; Vestergaard-Poulsen et al. 2009; Yasuda et al. 2010; Kraus et al. 2014; Lyden et al. 2014; Reid et al. 2016; De Giglio et al. 2018). Understanding how focal damage to neural hubs impacts other structures in the brain at the systems level is therefore an important step in understanding how brains recover from damage and the basic mechanisms of neural plasticity.

In the present report, we capitalize on a nonhuman primate model of the interoceptive-allostatic network (as specified by Kleckner et al. 2017) to evaluate how damage to one of its hubs, the anterior cingulate cortex (ACC), impacts the structure of 2 other major hubs, the insula and the amygdala. A great deal of research effort has been focused on determining the plasticity mechanisms leveraged in the circuits responsible for motor (e.g. Dimyan and Cohen 2011; Darling et al. 2018) and exteroceptive sensory processing (e.g. olfactory, Reichert and Schöpf 2018; visual, Baroncelli and Lunghi 2021; auditory, Ryugo 2015; and somatosensory, O'Leary et al. 1994). However, plasticity in interoceptive circuits (i.e. sensory circuits responsible for primary representation of the "internal" state of the body; (Craig 2002, 2003, 2009) has received comparatively far less attention. Given the recent increase in interest in interoception (Chen et al. 2021) and emerging theories about an interoceptive basis of broad neuropsychiatric dysfunction (Seth 2013; Khalsa et al. 2018; Bonaz et al. 2021), investigating the ways in which the brain responds to damage in putative hubs of interoceptive processing is of critical importance.

The interoceptive-allostatic network was specified by Kleckner et al. (2017) using a combination of tract-tracing studies in macaque monkeys and functional magnetic resonance imaging in humans, and is thought to support allostasis—defined as the process by which the brain predictively maintains bodily energy regulation (McEwen and Stellar 1993; Sterling 2012). A wide range of psychological functions rely on allostasis, including affective experience, memory, decision-making, and pain (Kleckner et al. 2017). The realization of this network in primates is likely to be substantially different from that in rodents, which are commonly used in laboratory studies of neuroplasticity (see Kolb and Gibb 2007 for a review of this literature highlighting the common use of rodent models). Specifically, the rodent nervous system includes different interoceptive pathways (e.g. direct projections from the parabrachial nucleus to insula not present in primates; Shipley and Sanders 1982; Pritchard et al. 2000), which lack both comparable complexity (Krockenberger et al. 2020) and connectivity (Evrard et al. 2014) to human or monkey interoceptive cortex. Rhesus monkeys (*Macaca mulatta*) share homologies in structure (Mesulam and Mufson 1985; Pitkänen and Kemppainen 2002; Freese and Amaral 2009; Evrard et al. 2014 ; Evrard 2019) and functional connectivity (Vincent et al. 2007; Touroutoglou et al. 2016) of the interoceptive-allostatic network. Beyond these anatomical homologies, rhesus monkeys share important similarities in behaviors thought to be dependent on interoceptive-allostatic network activity, including socio-affective processing (Phillips et al. 2014) and heart beat detection (Charbonneau et al. 2022).

Building on neuropsychological evidence from our group showing that large, selective lesions of interoceptive-allostatic neural hubs in adult rhesus monkeys resulted in relatively minimal changes to behaviors ostensibly dependent on activity in this network (Bliss-Moreau et al. 2021; Charbonneau et al. 2021), we evaluated plastic reorganization of cortical (insula) and subcortical (amygdala) structures following neurotoxic lesions of the ACC, as well as changes in an insula-adjacent control structure (the claustrum). Given the heterogeneity of structural and functional connectivity between subregions and nuclei in the primate insula (Evrard et al. 2014; Evrard 2019) and amygdala (Freese and Amaral 2009), respectively, we used stereological techniques on postmortem brains to obtain volumes across the 15 major subregions of the insula and the 6 main nuclei of the amygdala in monkeys with ACC lesions and neurologically intact control monkeys. Such experiments have the power to reveal important changes that occur in the primate interoceptive-allostatic network following damage—with both higher resolution and greater damage specificity than is possible in studies of human brain damage, while preserving critical homologies.

Materials and methods

All experimental procedures and methods were developed in collaboration with the veterinary staff at the California National Primate Research Center (CNPRC), approved by the University of California, Davis Institutional Animal Care and Use Committee, and were conducted in accordance with the National Institutes of Health guidelines for the use of animals in research.

Subjects and surgical procedures

A total of 13 adult (mean ± standard deviation, SD = 11.03 ± 2.41 years) male rhesus monkeys (*M. mulatta*) born at the California National Primate Research Center were studied. Seven monkeys received bilateral ibotenate lesions targeting the ACC, including the gyrus and ventral bank of the sulcus (i.e. Areas 24, 32, and 25 as defined by Vogt 2009; excluding the dorsal bank, which is considered a motor area; see Dum and Strick 2002). Lesioned subjects ($N = 7$) were the same as reported in (Bliss-Moreau et al. 2021). Six additional subjects served as controls and were from a series of different studies in our laboratory. Three of the 6 controls we report on here served as the "histologic controls"

in Bliss-Moreau et al. (2021) (i.e. not the monkeys who served as the control animals for the behavioral experiments as they were not euthanized at the conclusion of those experiments) for calculations of lesion extent. An additional 3 control subjects were selected from archival tissue to ensure that the same perfusion and staining protocols were used (see below) for the purposes of the present experiments. As the surgical procedures have been described in detail elsewhere (Bliss-Moreau et al. 2021), we summarize them briefly here.

Presurgical MRI

Prior to each surgery, MRI scanning was conducted using a 1.5 T Genesis Signa MRI Scanner (GE Healthcare) at the UC Davis Veterinary Medical Teaching Hospital. Monkeys were sedated with ketamine, placed in an MRI-compatible stereotaxic apparatus (Crist Instruments), and T1-weighted images were collected with a TR of 22 and a TE of 7.9. MRIs were used to plan coordinates of ibotenate injection sites during surgery.

Surgery

Monkeys were sedated with ketamine hydrochloride (10 mg/kg, i.m.), had their heads shaved, and were endotracheally intubated. A mix of isoflurane (~1%; mixed with oxygen and then medical grade air) and intravenous fentanyl (7–10 μg/kg/h) were used for anesthesia. Surgeries were completed while monkeys were placed in the same stereotaxic frame used during MRI scanning. A midline incision was made, and the skin, fascia, and muscle were separated into 3 layers before the outline of a single craniotomy (extending ~3-mm beyond the proposed AP and ML coordinates) was drawn onto the skull. A bone flap was removed, and the dura was opened along the AP and ML extents of the craniotomy. Ibotenate (catalog #0285, lots 26B/90,549 and 26C/100,306, Tocris Bioscience) was prepared for injection at a concentration of 10 μg/μL in 0.22-μm sterile filtered 0.1 M PBS. Initially, the entire left side was injected (caudal to rostral) followed by the entire right side (rostral to caudal); in later surgeries injections alternated between right and left moving caudal to rostral. Between 19 and 23 injections were performed per hemisphere. Following injections, the dura was moved into position to cover the brain and sutured where possible. Surgicel (Ethicon) and GelFoam (GE Healthcare) were placed over the brain and the bone flap was repositioned and secured with self-tapping bone screws (catalog #218–0201, #218–0217, #218–1604 using #220–0019, Osteomed) placed in titanium clips. Each anatomical layer was closed by suture and skin glue was applied. Monkeys were removed from the stereotaxic frame and recovered in the postoperative suite at the CNPRC. The lesion surgeries ranged in length from 15.5 to 22.75 h (mean = 17.6 h; SD = 2.48). They returned to their homerooms and were re-paired with their pair mate once recovered.

Histological procedures

Euthanasia was carried out by a board certified veterinary pathologist using 0.33-mL/kg Fatal-Plus (120-mg/kg sodium pentobarbital; Vortech Pharmaceuticals, Dearborn, MI). The mean duration of time between the lesion surgeries and sacrifice was 3.83 years (SD = 0.19). Histologic and immunohistological processing were performed according to methods previously published (Lavenex et al. 2009; Bliss-Moreau et al. 2017, 2021). Monkeys were perfused transcardially with 1% paraformaldehyde (PFA) in 0.1-M sodium phosphate buffer at 4°C at a rate of 250 mL/min for 2 min followed by 4% PFA at a rate of 250 mL/10 min. For the last 50 min of the perfusion, the perfusion rate of 4% PFA was increased to 100 mL/min. Brains were blocked caudal to the corpus callosum in the occipital lobe, extracted from the skull, and placed in 4% PFA for a 6-h postfix. Following this, brains were cryoprotected by immersion in 10% glycerin with 2% dimethylsulfoxide (DMSO) in 0.1-M sodium phosphate buffer for 24 h, then 20% glycerin with 2% DMSO in 0.1 M sodium phosphate buffer for 72 h; all incubations were at 4°C. Brains were then frozen in 2-methylbutane within a dry ice and ethanol bath. Coronal sections were cut with a freezing sliding microtome (Microm HM 440; Microm Int. GmbH, Walldorf, Germany) into either 6 series at 30 μm and 1 series at 60 μm or 8 series all at 30 μm. One series (the 60-μm series, when available) was used for Nissl staining. These sections were collected in 10% buffered formaldehyde and stored at 4°C for 2 weeks. Tissue was then rinsed twice in 0.1-M sodium phosphate buffer and sections were mounted onto gelatin-coated glass slides and dried overnight. Dried sections were placed in a 1:1 mixture of chloroform and ethanol for 2 h, then in a fresh mixture of 1:1 chloroform and ethanol for another 2 h, and were finally partially hydrated and left at 37°C overnight. Sections were stained in 0.25% thionin (Thermo Fisher Scientific) for 35 s then dehydrated, decolored, cleared in xylene, and coverslipped with DPX Mountant (Electron Microscopy Sciences).

Lesion evaluation

Evaluation of the ACC lesions was described in detail in Bliss–Moreau et al. (2021). In short, the Nissl series and an additional series stained for SMI-32 (to stain for neurons) immunohistochemistry were scanned using a TissueScopeLE scanner (Huron Digital Pathology, St. Jacobs, Ontario, Canada) and imported into StereoInvestigator (version 2020.1.3, MBF Bioscience) for offline analysis. Lesion estimation and volume estimation (for the 3 brains used as histologic controls in Bliss-Moreau et al. 2021) were conducted on sections every 240 μm. Areas 24, 32, and 25 were traced on Nissl-stained sections in control cases according to cytoarchitectonics defined by Vogt et al. (2005). Areas were traced in lesion cases only where cells were present and the layering of cortex was intact, with corresponding SMI-32 sections available to augment the Nissl images during tracing when boundaries were not obvious on the Nissl images. Volumes were estimated using the Cavilieri estimator (Gundersen and Jensen 1987) in StereoInvestigator with a grid size of 100 × 100 μm and a z-interval of 480 μm. Lesion extent was determined by dividing individual lesion case volumes by the average volume of the 3 histologic controls. Individual descriptions of the lesions, including descriptions of extraneous damage to surrounding cortex, are reported in Bliss-Moreau et al. (2021). Mean Area 24 damage was 79.6% (SD = 14.4%); mean Area 32 damage was 35.9% (SD = 26.4%) across all cases and 41.8% (SD = 23.5%) excluding Case A where Area 32 was spared; and mean Area 25 damage was 55.3% (SD = 21.9%). Individual case volumes are reported in Table 1. Representations of the lesions and examples of damage are shown in Fig. 1 (adapted from Bliss-Moreau et al. 2021).

Stereological analyses of the amygdala and insula

Stereological volume estimations were performed offline with StereoInvestigator (version 2020.1.3, MBF Bioscience). Relevant slides, including 2–3 slides on either side of the most anterior and posterior portions of the structure were scanned using a TissueScope scanner (Huron Digital Pathology). We estimated the volume of the whole amygdala, the volumes of the main amygdala nuclei (lateral, basal, paralaminar, accessory basal, central, and medial as defined by Price et al. 1987; Freese and Amaral 2009; Supplementary Fig. S1, see online supplementary material for a

Table 1. Volume of ACC subregions in ACC-lesioned animals and controls.

	Area 24				Area 32				Area 25			
	Left volume	Right volume	Left atrophy	Right atrophy	Left volume	Right volume	Left atrophy	Right atrophy	Left volume	Right volume	Left atrophy	Right atrophy
Control animals												
Control 1	211.78	216.07			63.04	62.64			20.54	19.30		
Control 2	275.77	258.80			64.62	83.63			24.34	22.14		
Control 3	205.52	224.35			47.99	46.13			30.43	30.77		
Control average	230.88	233.07			58.55	64.13			25.10	24.07		
ACC-lesioned animals												
Case A	130.83	99.24	43.33%	57.42%	85.91	83.78	0%	0%	18.89	20.81	24.77%	13.57%
Case B	63.69	54.40	72.43%	76.66%	46.26	45.65	21.00%	22.03%	2.09	8.12	91.67%	66.26%
Case C	12.61	13.54	94.54%	94.19%	29.83	24.03	49.06%	62.53%	7.13	8.06	71.60%	66.51%
Case D	22.99	43.32	90.04%	81.41%	37.06	50.10	36.71%	21.88%	17.06	10.01	32.05%	58.41%
Case E	23.11	20.29	89.99%	91.29%	18.56	18.71	68.31%	70.83%	7.39	5.34	70.55%	77.82%
Case F	41.10	25.64	82.20%	89.00%	25.49	20.99	56.46%	67.27%	8.76	15.45	65.12%	35.84%
Case G	40.12	72.99	82.62%	68.68%	44.15	63.40	24.59%	1.15%	17.30	7.50	31.08%	68.82%
Lesioned average	*47.78*	*47.06*	*79.31%*	*79.81%*	*41.04*	*43.81*	*36.59%*	*35.10%*	*11.23*	*10.76*	*55.26%*	*55.32%*

Note: Volumes are in cubic millimeters. Three of the 6 controls were used to quantify lesion extent as reported in Bliss-Moreau et al. (2021). The additional three controls were added for the purposes of the present comparisons and were not used at the time that lesion extent was calculated for our previous publication. Average values for each group (control animals and ACC-lesioned animals) are shown in italics.

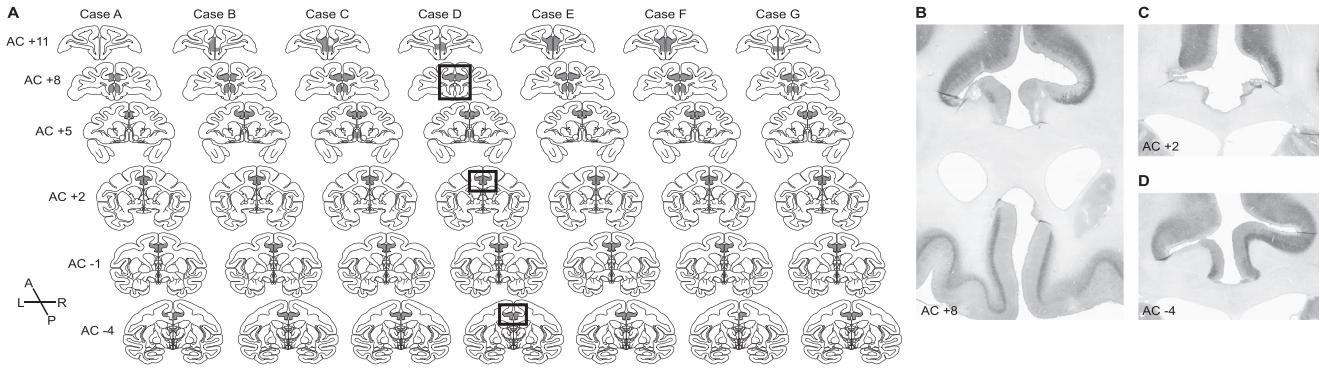

Fig. 1. Representations of lesion extent (dark gray) were made by overlaying the StereoInvestigator tracings over templates for the macaque brain, which were made using http://braininfo.rprc.washington.edu/PrimateBrainMaps/atlas/Mapcorindex.html. Each column in A) shows a separate monkey, with cases corresponding to the case names in Table 1. Coronal sections are arranged from rostral (top) to caudal (bottom). Sections are separated by 3 mm, and the distance from the anterior commissure (AC) is indicated (e.g. AC +2 is ∼2-mm rostral to the AC and AC −4 is ∼4-mm caudal to the AC). Panels B)–D) show examples of SMI-32 immunohistochemistry scanned images from case D (identified with rectangles in panel A), which were used for evaluation of the lesion area for each 30 μm section.

color version of this figure), and the volume of the 15 insula subregions (granular dorsal [Igd], granular ventral [Igv], dorsal fundus posterior [Idfp], dorsal fundus anterior [Idfa], dysgranular dorsal [Idd], dysgranular mound [Idm], dysgranular ventral [Idv], ventral fundus posterior [Ivfp], ventral fundus anterior [Ivfa], agranular posterior-lateral [Iapl], agranular posterior [Iap], agranular lateral [Ial], agranular intermediate [Iai], agranular medial [Iam], and agranular posterior-medial [Iapm] as defined by Carmichael and Price 1994; Evrard et al. 2014; Supplementary Fig. S2, see online supplementary material for a color version of this figure) according to the Cavalieri principle (Gundersen and Jensen 1987). About 16 sections per animal (480-μm apart) were used for the measurements of the amygdala. About 22 sections per animal (960-μm apart) were used for the measurements of the insula. Volumes were obtained for all structures bilaterally. Tracings for volume estimations were all completed blind to lesion condition (slides were scanned and labeled by a separate experimenter than the one who carried out the tracings) and carried out by the first author. In addition, the images of all right hemisphere structures were horizontally inverted such that tracings could also be done blind to hemisphere and any lateralized effects observed would not be attributable to tracing biases. Prior to collecting data for the present experiments anatomical boundaries were reviewed on several cases for both the insula and amygdala and decisions about these boundaries were reached by consensus of 3 authors.

Stereological analysis of the claustrum

To give confidence to our findings in the insula, we also performed stereological volume estimations of the claustrum to serve as a "control" region. The claustrum was selected because it is physically proximate to the insula, has clear anatomical boundaries, and is not a hub in the interoceptive-allostatic network. As with insula volume estimations, ∼22 sections per animal (960-μm apart) were used and tracings were accomplished blind to lesion condition and hemisphere after experimenters reached a mutual consensus about structural boundaries.

Volume estimation by MRI

After histological evaluation, we returned post hoc to preoperative MRIs for the ACC-lesioned animals to compute their pre-lesion insula volumes. This allowed us to determine whether there were hemispheric differences within animals prior to surgery. We

computed volumes using the T1-weighted images acquired for the planning of the lesion surgeries (described above) by hand-tracing insula regions-of-interest in each subject's data using ITK-SNAP (version 3.8.0; Yushkevich et al. 2006) on consecutive coronal slices. The cytoarchitectonic differentiation of individual subregions was not possible on MRI and so only whole structure volumes were computed. The anterior extent of the insula was specified as the slice that included the anterior end of the putamen. The posterior boundary of the insula was specified as the slice that included the posterior end of the superior limiting sulcus (where the superior limiting and inferior limiting sulci meet to form the lateral sulcus). The dorsal and ventral boundaries were specified by drawing a line tangentially through the fundi of the superior and inferior limiting sulci, respectively. We did not compute preoperative amygdala volumes because there were no significant effects of lesion condition on whole amygdala volume in the histological data and nuclei could not be reliably identified on the available MRIs.

Statistical analyses

Statistical analyses were performed in R version 4.0.4 (R Core Team 2019). Linear mixed-effects models (implemented using the *lmer* function from the package *lme4*; Bates et al. 2015) were used to analyze lesion group differences in amygdala, insula, and claustrum volumes. For all 3 structures, we first assessed models in which lesion condition, hemisphere, and their interaction were entered as predictors of whole structure volume with individual monkey as a random effect (whole structure models). We then evaluated the role of the different nuclei (for the amygdala) and subregions (for the insula) by also including nucleus/subregion as a fixed effect, two 2-way interactions (nucleus/subregion × lesion condition and nucleus/subregion × hemisphere), the 3-way interaction between nucleus/subregion × lesion condition × hemisphere, and subregion nested within individual monkey as a random effect (subregion models). Relative amygdala nuclei volumes were computed by dividing the volumes of individual nuclei by the whole structure volume for each monkey because the amygdala contains a large volume of cells, which do not belong to the 6 main nuclei (whereas insula subregions sum to the total insula volume). We evaluated lesion group differences in relative amygdala volumes using an identically structured model to the subregion models described above. Follow-up models for the insula were also conducted in which only granular (i.e. Igd, Igv, Idfp, and Idfa), dysgranular (i.e. Idd, Idm, Idv, and Ivfp), or agranular (i.e. Ivfa, Iapl, Iap, Iapm, Ial, Iai, and Iam) subregions were included. These models had an identical structure to the subregion models previously described.

To test the interaction contrasts for subregion models, we used the *joint_tests* function from the *emmeans* package (Lenth 2021). The *joint_tests* function obtains and tests the interaction contrasts for all effects in the model, with separate tables obtained at each level of a particular factor (i.e. to assess effects of hemisphere and lesion condition, and their interaction, at the level of each subregion to determine the source of any effects seen at the whole structure level). The function computes an *F*-statistic and is based on the estimated marginal means (rather than model coefficients). All analyses are robust to unequal sample sizes (Snijders 2005).

As per field standards, $\alpha = 0.05$ was defined as the level of significance and *P*-values that are <0.05 are reported out as significant. For the sake of completeness, however, we report out instances in which α did not reach the conventional level of significance but which might be indicative of meaningful effects (i.e. $0.05 \leq P \leq 0.10$) that did not reach the conventional level of significance because of the small sample size. In these cases, we do not indicate that the effects are significant, but we do note that they may nonetheless represent potential effects. In cases where $P > 0.1$, we indicate that effects are not significant.

Results

The impact of ACC damage on amygdala volume

Stereological estimates of the volumes of the 6 main amygdala nuclei (i.e. lateral, basal, accessory basal, central, medial, and paralaminar) as well as the whole structure volumes were computed. First, we assessed whether there were lesion group differences in the absolute (i.e. raw) volumes of the entire amygdala and then its component nuclei.

The impact of ACC damage on raw amygdala whole structure and nuclei volumes

Neither lesion condition ($\chi^2(1) = 0.24$, $P = 0.62$) nor hemisphere ($\chi^2(1) = 0.16$, $P = 0.69$) were significant predictors of whole amygdala volume. The interaction between lesion condition and hemisphere was also not significant ($\chi^2(1) = 2.01$, $P = 0.15$). See Fig. 2A.

Lesion condition ($\chi^2(1) = 0.77$, $P = 0.38$), hemisphere ($\chi^2(1) = 0.73$, $P = 0.12$), and the interaction between lesion condition and hemisphere ($\chi^2(1) = 1.58$, $P = 0.21$) were also not significant predictors when individual nuclei volumes were analyzed. The 2-way interaction between lesion group and nucleus ($\chi^2(5) = 0.94$, $P = 0.97$) and the 3-way interaction between lesion group, nucleus, and hemisphere ($\chi^2(5) = 3.40$, $P = 0.64$) were also not significant. There was a significant effect of nucleus ($\chi^2(5) = 1{,}102.72$, $P < 0.001$), indicating that in both lesioned brains and control brains there were significant differences in volume between individual nuclei, as expected. There was also a significant interaction between hemisphere and subregion ($\chi^2(5) = 21.17$, $P < 0.001$), indicating that nuclei volumes varied across the left and right hemispheres in both lesioned and control brains. When assessing the effect of hemisphere at the level of each nucleus, we found a significant impact of hemisphere on accessory basal nucleus volume ($F(1, 66) = 16.71$, $P < 0.001$). Accessory basal nucleus volumes were significantly greater in the right hemisphere than the left hemisphere. The effect of hemisphere on lateral nucleus volume ($F(1, 66) = 3.25$, $P = 0.08$), suggested a potential impact of hemisphere with greater volumes in the left, as compared with the right, hemisphere. There was not a significant effect of hemisphere on any of the other nuclei volumes (all $P > 0.20$). See Fig. 2B.

The impact of ACC damage on relative amygdala nuclei volumes

The whole amygdala includes a large volume of neurons and other cells outside of the specific nuclei analyzed here. As such, we analyzed relative nucleus volumes by computing the volumes of specific nuclei as a percentage of the whole structure volume in each monkey, consistent with previous analyses (Chareyron et al. 2011). There was no main effect of lesion group on relative amygdala nuclei volumes ($\chi^2(1) = 0.00$, $P = 1.00$) nor was there a significant interaction between lesion group and hemisphere ($\chi^2(1) = 0.00$, $P = 1.00$). The interaction between lesion group and nucleus, however, suggested potential group differences in some individual nuclei ($\chi^2(5) = 10.42$, $P = 0.06$). The interaction between hemisphere and nucleus was significant ($\chi^2(5) = 26.69$, $P < 0.001$), as was the case in the absolute volume data reported above. To follow up on the potential interaction between lesion group and nucleus and the interaction between hemisphere and nucleus,

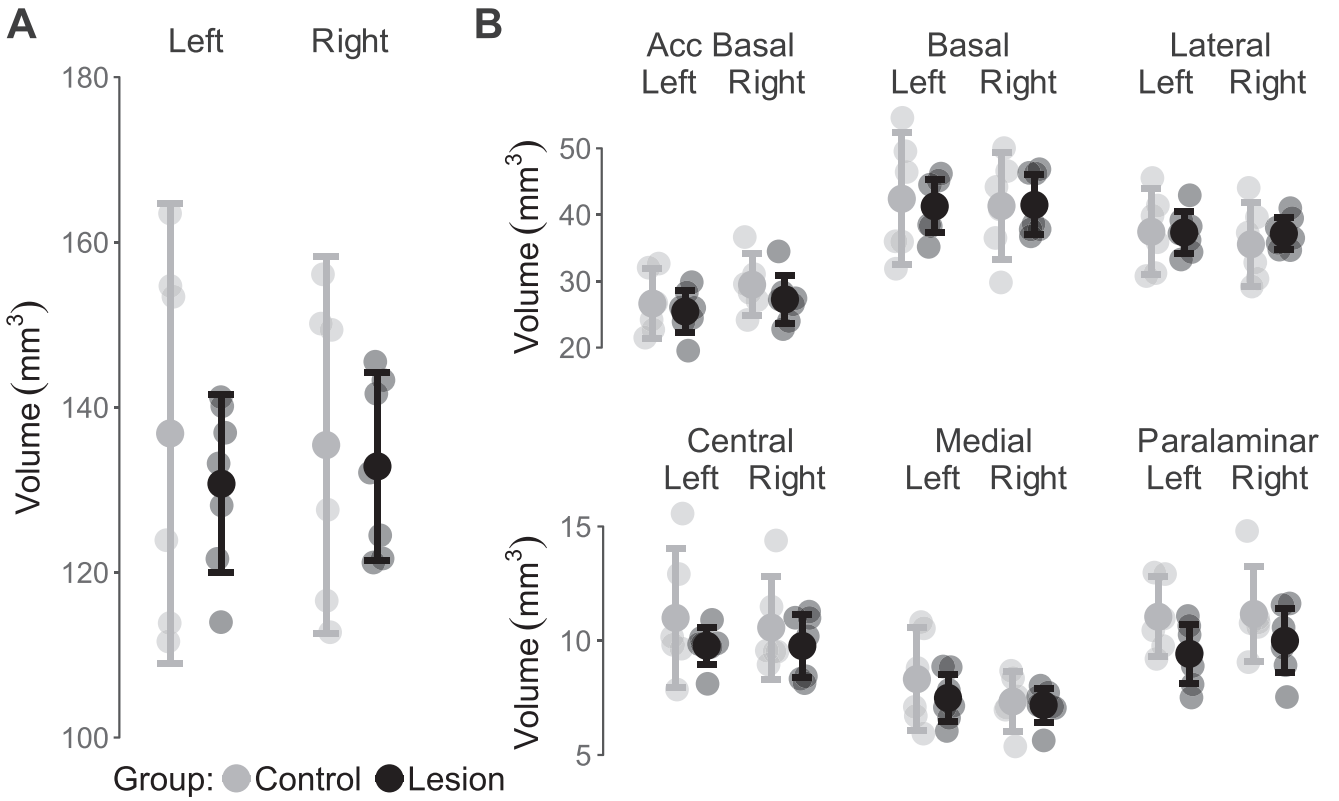

Fig. 2. Absolute volumes of the A) whole amygdala and B) 6 main nuclei of the amygdala. Volumes are in cubic millimeters. Left and right hemisphere data are disaggregated. All individual data points are shown as well as means and adjusted 95% confidence intervals (CI). Control volumes are shown in gray and lesioned volumes are shown in black.

we evaluated the impact of lesion group, hemisphere, and a lesion group X hemisphere interaction in each nucleus. We found that lesion group was a significant predictor of relative lateral nucleus volume ($F(1, 66) = 5.36$, $P = 0.02$), such that relative lateral nucleus volumes were significantly greater in lesioned, as compared with control, monkeys. This finding is consistent with the findings of Chareyron et al. (2016), which report on lateral nucleus expansion after neonatal hippocampal lesions. There was also a significant effect of hemisphere on relative lateral nucleus volumes ($F(1, 66) = 5.41$, $P = 0.02$) such that relative lateral nucleus volumes were significantly greater in the left hemisphere as compared with the right hemisphere. The interaction between lesion group and hemisphere for lateral nucleus volumes was not significant ($F(1, 66) = 0.77$, $P = 0.38$), indicating the effect of lesion condition was comparable across hemispheres. This analysis also suggested a potential lesion group X hemisphere interaction for relative accessory basal nucleus volume ($F(1, 66) = 2.81$, $P = 0.10$) such that lesioned and control subjects had similar left hemisphere volumes but control subjects had larger right hemisphere volumes. Comparison across nuclei again revealed an effect of hemisphere on relative accessory basal nucleus volume ($F(1, 66) = 19.58$, $P < 0.001$), with significantly larger relative volumes in the right, as compared with the left, hemisphere. The effects of hemisphere and lesion group were not significant for any other nucleus (all $P > 0.17$). See Fig. 3.

The impact of ACC damage on insula volume

Our second target of evaluation was the insula because, like the amygdala, it has robust reciprocal connections with the ACC and is also a major hub in the interoceptive-allostatic network. We first assessed lesion group differences in absolute whole structure volumes and then assessed differences at the level of the 15 consistently identifiable subregions (Evrard et al. 2014).

There was a significant effect of hemisphere ($\chi^2(1) = 10.31$, $P = 0.001$) on total insula volume as well as a significant lesion condition X hemisphere interaction ($\chi^2(1) = 6.47$, $P = 0.01$). Although right and left insula volumes were comparable in lesioned subjects, there were volumetric differences between the hemispheres in control animals. Control animals had larger right, as compared to left, insulas. See Fig. 4A.

We next included subregions in our model to assess any impacts of subregion that might be driving the significant lesion group X hemisphere interaction in the model assessing whole insula volumes. This model revealed the expected main effect of subregion ($\chi^2(14) = 1{,}916.08$, $P < 0.001$), indicating that some subregions were significantly larger than others. We also found a significant main effect of hemisphere ($\chi^2(1) = 8.61$, $P = 0.003$), as well as the same lesion group X hemisphere interaction ($\chi^2(1) = 5.41$, $P = 0.02$) as we had seen in the whole structure model. In addition to the significant lesion group X hemisphere interaction, we also found a significant 3-way interaction between lesion group, hemisphere, and subregion ($\chi^2(14) = 33.60$, $P = 0.002$). Evaluation of the means revealed that agranular subregions may have been driving the interaction; control animals had larger right, as compared with left, agranular volumes and lesioned animals had comparable volumes on the right and left sides. This pattern was not obvious in dysgranular or granular subregions, although these subregions appeared to potentially be larger in lesioned animals relative to controls. See Fig. 4B.

To explore the 3-way interaction between lesion group, hemisphere, and subregion, we constructed 3 different models—one for each the granular, dysgranular, and agranular subregions

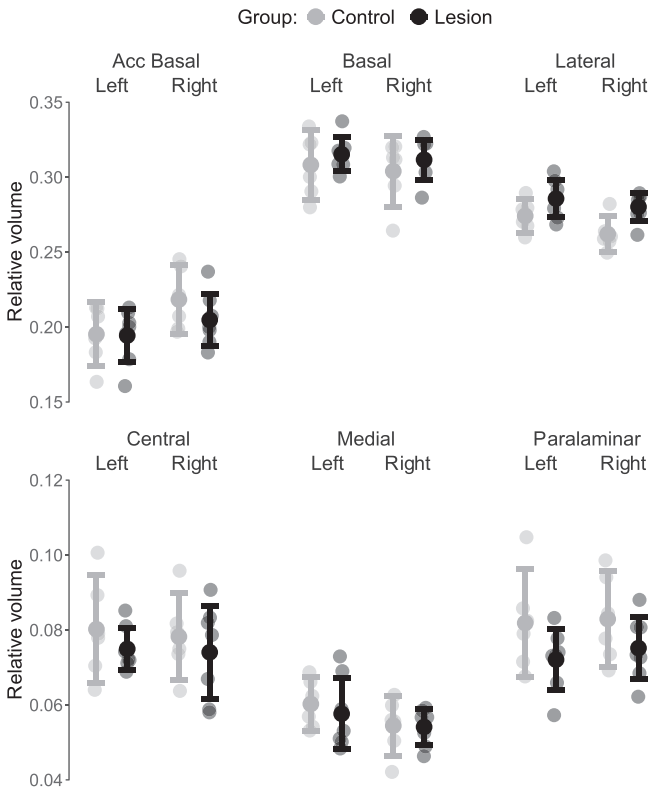

Fig. 3. Relative volumes of the 6 main nuclei of the amygdala. Relative volumes were calculated by dividing the absolute volume of an individual nucleus by the absolute volume of the whole amygdala. All individual data points are shown as well as means and adjusted 95% CI. Control volumes are shown in gray and lesioned volumes are shown in black.

respectively. For granular subregions (Igd, Igv, Idfp, and Idfa), subregion was a significant predictor of volume ($\chi^2(3) = 481.57$, $P < 0.001$) as expected, indicating differences in volumes across subregions. The group X hemisphere interaction suggested a potential effect ($\chi^2(1) = 3.02$, $P = 0.08$). Evaluation of the means indicated that controls had comparable right and left hemisphere granular region volumes, whereas lesioned subjects had greater right, as compared with left, hemisphere granular insula volumes, potentially contributing to the overall pattern seen at the level of the whole structure. The model predicting dysgranular subregion volumes revealed a significant main effect of subregion ($\chi^2(3) = 565.27$, $P < 0.001$), but no lesion group X hemisphere interaction ($\chi^2(1) = 0.08$, $P = 0.78$). Finally, the agranular model revealed significant main effects of subregion ($\chi^2(6) = 201.82$, $P < 0.001$) and hemisphere ($\chi^2(1) = 8.61$, $P = 0.003$). The interaction between lesion group and hemisphere was also significant ($\chi^2(1) = 12.14$, $P < 0.001$), as was the 3-way interaction between lesion group, hemisphere, and subregion ($\chi^2(6) = 17.62$, $P = 0.007$), suggesting that the lesion group X hemisphere interaction seen at the level of the whole structure was likely being driven by differences in agranular insula volumes, consistent with the data visualization. Analysis at the level of each subregion for the agranular model revealed significant group X hemisphere interactions for Iai ($F(1, 77) = 11.65$, $P = 0.001$), Ial ($F(1, 77) = 12.16$, $P < 0.001$), and Iam ($F(1, 66) = 4.79$, $P = 0.03$). For all 3 of these subregions, lesioned subjects had similar volumes across hemispheres and control subjects had greater right, compared with the left, hemisphere volumes. As such, these 3 regions in the ventral anterior insula appeared to be the main regions driving the lesion group X hemisphere interaction seen at the level of the whole insula and at the level of the agranular insula. Although right hemisphere volumes were comparable or even smaller (although not significantly) in lesioned subjects across these regions of the ventral anterior insula, in the left hemisphere lesioned subjects had larger volumes than control subjects, likely primarily driving the significant group difference in left insula volume when the whole structure volume was analyzed (see Fig. 4A). The group X hemisphere interaction was not significant for Iap, Iapl, Iapm, or Ivfa (all $P > 0.40$). Figure 4C shows agranular insula volumes by subregion.

To determine whether the observed lesion group X hemisphere interaction was a real effect or merely the result of nonrandom sampling relative to insula structures prior to surgery (i.e. we happened to select control monkeys with smaller left, as compared with right, insulas) we carried out an analysis of our preoperative MRI data for lesioned subjects. This analysis considered whole insula volumes only because there was no way to determine subregions on the MRIs that we had available. Volumes were computed from hand-traced regions-of-interest for all lesioned subjects. Volumes of the insula derived from preoperative MRI data and histological analyses were highly correlated ($r(12) = 0.87$, $P < 0.001$). We compared left and right insula volumes using a 1-tailed paired t-test, using our histological data as the basis for the directional assumption (i.e. right > left, as seen in the stereological volumes from control subjects). This test suggested a potential asymmetry ($t(6) = -1.69$, $P = 0.07$), which failed to reach the conventional level of significance but resulted in a medium to large effect size (Cohen's $d = 0.64$). This suggests that the hemispheric asymmetry seen in control subjects may have been present in lesioned subject prior to surgery and that neural reorganization following lesions may have resulted in left insula volume increases. Preoperative insula volumes are shown in Fig. 5A. Figure 5B and C show the correlation between MRI and histological volumes by hemisphere.

Claustrum

We assessed claustrum volumes as a control region. ACC-lesioned monkeys and control monkeys had comparable left (ACC-lesioned: mean ± SD = 622.04 ± 89.25 mm^3; control: mean ± SD = 557.11 ± 108.19 mm^3) and right (ACC-lesioned: mean ± SD = 641.73 ± 91.72 mm^3; control: mean ± SD = 560.03 ± 119.00 mm^3) claustrum volumes. Neither lesion condition ($\chi^2(1) = 2.30$, $P = 0.13$) or hemisphere ($\chi^2(1) = 2.08$, $P = 0.15$) were significant predictors of claustrum volume. The interaction between lesion group and hemisphere ($\chi^2(1) = 1.02$, $P = 0.31$) was also not significant, suggesting that the lesion group X hemisphere interaction seen in the insula was not due to some global change in that general region of the brain (or the brain at large), but was rather localized to the insula specifically.

Correlations with ACC atrophy

The histological analyses demonstrate volumetric differences related to lesion group in the left and right lateral nucleus of the amygdala as well as in the left insula, most strikingly in its agranular portion. To evaluate the possibility that these differences might be related to damage in particular regions of the ACC, we correlated these region volumes with ACC atrophy. No clear pattern emerged in these analyses. Only the right lateral nucleus volume and lesion extent in right ACC area 25 were significantly correlated ($r(5) = -0.84$, $P = 0.01$). There was also a potential relationship between right lateral nucleus volume and left ACC Area 32 lesion extent ($r(5) = -0.69$, $P = 0.08$) and left ACC

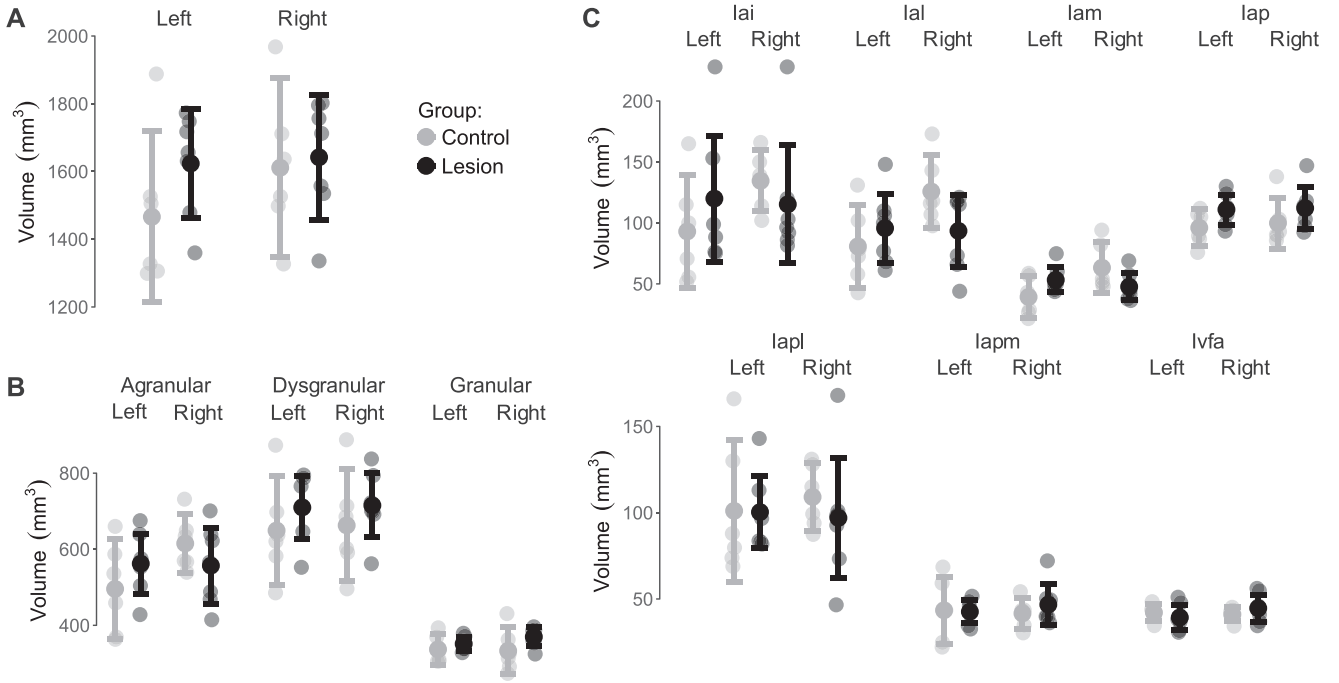

Fig. 4. Absolute volumes of the A) whole insula, B) main cytoarchitectonic regions of the insula (agranular, dysgranular, and granular), and C) agranular insula subregions (ventral fundus anterior [Ivfa], agranular posterior-lateral [Iapl], agranular posterior [Iap], agranular lateral [Ial], agranular intermediate [Iai], agranular medial [Iam], and agranular posterior-medial [Iapm]). Volumes are in cubic millimeters. All individual data points are shown as well as means and adjusted 95% CI. Control volumes are shown in gray and lesioned volumes are shown in black.

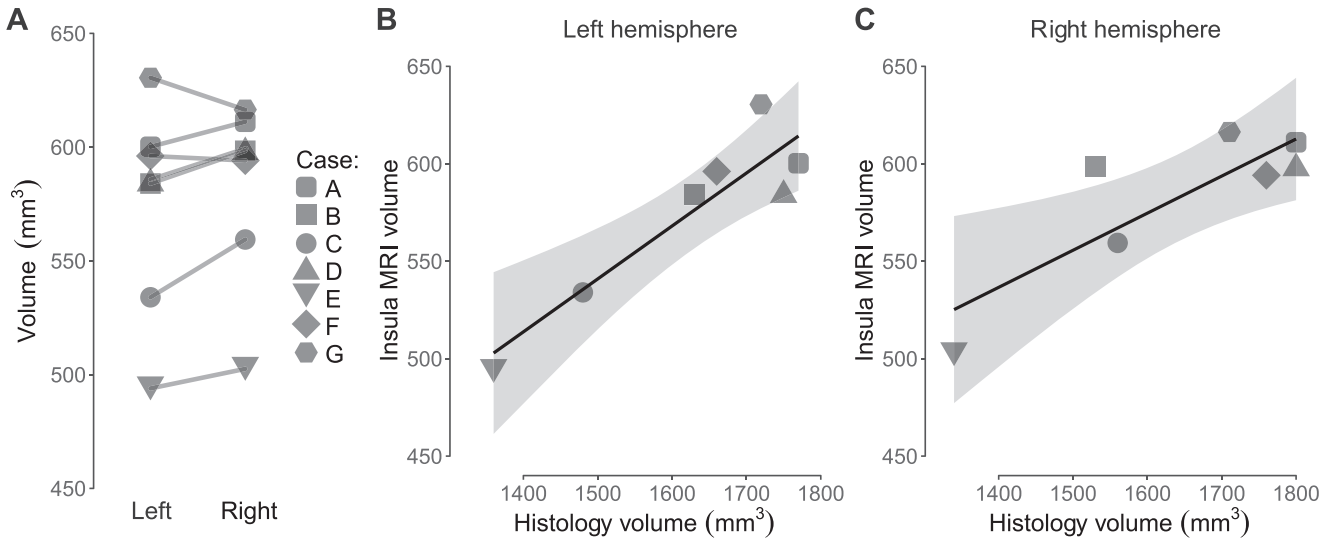

Fig. 5. MRI evaluation of preoperative insula volumes in lesioned subjects. A) Whole insula volumes for each lesioned subject in the left and right hemispheres. Each case is differentiated with a different shape marker. B–C) correlations between insula volumes as estimated from MRI and volumes as estimated from histology for the left B) and right C) insula.

Area 24 lesion extent ($r(5) = -0.69$, $P = 0.08$). Given the number of correlations that were not significant and the relatively small samples, the extent to which these relationships (and lack thereof) are reflective of actual neural relationships is not clear and a fruitful avenue for future study.

Discussion

Our results demonstrate that damage to the ACC in adult monkeys led to significant and specific reorganization in other interoceptive–allostatic network hubs—the amygdala and the insula—when these structures were assessed several years after ACC damage. Relative to neurologically intact control monkeys, monkeys who received selective neurotoxic lesions of the ACC had larger lateral amygdala nuclei (considered relative to overall amygdala size). Monkeys with ACC lesions also had expanded ventral anterior insulas in the left hemisphere, with the most notable group differences occurring in the agranular lateral (Ial), agranular intermediate (Iai), and agranular medial (Iam) subregions (although it is possible that more subtle changes throughout the structure contributed to lesion group differences seen in whole insula volume in the left hemisphere). There were no effects of lesions on volumes in a control region proximate to the insula, the claustrum, suggesting that the changes observed

in amygdala and insula were not due to global brain-wide reorganization, but instead specific to regions networked with the ACC. The fact that these changes were expansion, rather than atrophy, of particular regions within each the amygdala and the insula suggests that such changes may be compensatory to preserve function following damage, although future studies are needed to determine if this is the case. By obtaining unbiased stereological volume estimates from postmortem tissue, we were able to pinpoint the precise regions that reorganized following lesions, with greater specificity than would be possible using lower-resolution methods like MRI.

Our results suggest that much like exteroceptive sensory circuits in the brain (e.g. O'Leary et al. 1994; Ryugo 2015; Reichert and Schöpf 2018; Baroncelli and Lunghi 2021), interoceptive sensory circuits are also capable of significant plasticity following damage. The interoceptive-allostatic network that we investigated here provides a critical link between central nervous system representations of interoceptive sensations and the regulation of peripheral systems in the body—which supports domain-general psychological functions not limited to interoception, reward, and decision-making (Kleckner et al. 2017). This network has 2 component intrinsic networks with overlapping neural hubs—the default mode and salience networks (Seeley et al. 2007; Touroutoglou et al. 2012; Raichle 2015; Kleckner et al. 2017), which are individually now thought to also contribute to domain-general processing (Barrett and Satpute 2013). Emerging evidence indicates that interoceptive-allostatic network activity, specifically, is perturbed both in individuals with mild cognitive impairment (Bateman et al. 2021) and patients with behavioral variant frontotemporal dementia (Birba et al. 2022), demonstrating that in addition to helping further our understanding of the ways in which the primate brain responds to damage, characterizing plastic potential in this network may have important implications for treating disorders like Alzheimer's disease and related dementias.

Reorganization in the amygdala

We found that the volumes of the lateral nuclei of the amygdala were significantly larger relative to whole amygdala volume in ACC-lesioned monkeys as compared with control monkeys. Notably, the lateral and basal nuclei are the main recipients of projections from the ACC (namely, Areas 24 and 25, targeted in our lesions) to the amygdala (Pandya et al. 1973; Amaral and Insausti 1992; Stefanacci and Amaral 2000, 2002; Freese and Amaral 2009) and these nuclei are also the primary origins, along with the accessory basal nucleus, of projections from the amygdala back to the cingulate (Porrino et al. 1981; Amaral and Price 1984; Vogt and Pandya 1987; Freese and Amaral 2009). It is therefore unsurprising that when we evaluated changes across the main nuclei of the amygdala, the lateral nucleus showed significant differences across groups, whereas other nuclei did not differ. Although we did not detect significant changes to the basal nucleus following ACC lesions, relative basal nucleus volumes were also greater in lesioned monkeys compared to controls. Our findings are potentially consistent with the observation that both neonatal and adult hippocampal lesions increase the number of mature neurons in the lateral nucleus of the monkey amygdala, with increases across the rostrocaudal extent of the nucleus in neonate-lesioned monkeys and increases restricted to the rostral portion in adult-lesioned monkeys (Chareyron et al. 2016)—suggesting that the lateral nucleus might be particularly plastic. As such, it is possible that the changes that we saw in the lateral nucleus of monkeys with ACC lesions may also reflect an increase in the number of mature neurons, although this will need to be confirmed in future investigations. One hypothesis, also to be explored in future studies, is that immature neurons from the paralaminar nucleus of the amygdala migrate to the lateral nucleus following insult to regions connected to it (Chareyron et al. 2016). The paralaminar nucleus of the amygdala is known to contain a large population of immature neurons both in monkeys (Chareyron et al. 2011; deCampo and Fudge 2012; Fudge et al. 2012) and humans (Yachnis et al. 2000). Many of these immature neurons persist into adulthood without differentiation (Chareyron et al. 2011, 2016) and the migration and maturation of these immature neurons from the paralaminar nucleus into other amygdala nuclei appears to be a critical feature of typical neural development in humans (Avino et al. 2018). Furthermore, the amygdala may be a region that receives newly generated neurons through adulthood, as revealed by simultaneous injections of BrdUrd and immunostaining for molecular markers of neurogenesis in adult monkeys (Bernier et al. 2002), providing another hypothesis to be explored in future work.

An alternative interpretation of our findings that lesioned animals had relatively larger lateral amygdala nucleus volumes is that the lateral nucleus may have uniquely (compared with other nuclei of the amygdala) maintained its size following ACC damage, whereas the remainder (or at least other portions) of the amygdala decreased in size. Although there were not significant lesion group differences in the mean whole amygdala volumes, mean volumes were lower in the lesioned group and it is possible that we did not have sufficient statistical power to detect a group difference. Across the 6 main nuclei, relative volumes were lower bilaterally in the lesioned group for the accessory basal, central, medial, and paralaminar nuclei (although these were not statistically significant) and higher bilaterally in the lesioned group for the basal and lateral nuclei. Given that these 2 nuclei are the primary origins and targets of connections with the ACC (Pandya et al. 1973; Porrino et al. 1981; Amaral and Price 1984; Vogt and Pandya 1987; Amaral and Insausti 1992; Stefanacci and Amaral 2000, 2002; Freese and Amaral 2009), this alternative interpretation of the pattern of results is also consistent with established neuroanatomical features of the interoceptive-allostatic network. Future studies will be necessary to determine the cellular dynamics, which gave rise to this pattern of results and which may confer some protective plastic potential to the lateral nucleus.

Changes to the volumes of particular regions of the amygdala—and specifically the lateral nucleus—have been found in a variety of contexts which suggest that the plastic nature of this structure has critical functional implications. People with major depressive disorder treated by electroconvulsive therapy showed significant expansion of the basolateral amygdala (as determined through MRI) and such expansion was associated with improved scores on the Quick Inventory of Depressive Symptomatology (Joshi et al. 2016; note that differentiation of basal and lateral nuclei on MRIs is difficult or impossible under most scanning parameters). Changes in lateral nucleus volume, specifically, have also been shown to mediate the association between PTSD symptoms both in the short-term (4–5 months post-trauma) and long-term (24–36 months post-trauma; Ousdal et al. 2020). Differences in lateral nucleus volumes have also been associated with several other neuropsychiatric disorders including schizophrenia (Barth et al. 2021) and psychosis (Armio et al. 2020). In laboratory experiments, rodents exposed to prenatal stress have larger lateral nuclei than rodents not exposed to prenatal stress (Salm et al. 2004). Taken together, these results, in concert with our own, indicate that the lateral nucleus appears to have particularly high plastic potential

and environmental influences can drive structural expansion with functional implications for affective processing. It is therefore unsurprising that following damage to the ACC, a portion of the brain with which the lateral nucleus is tightly networked, this nucleus of the amygdala undergoes changes which may preserve function in their shared networks.

Reorganization in the insula

In addition to causing relative expansion of the lateral nucleus of the amygdala, our findings demonstrate that damage to the ACC also causes selective expansion of the ventral anterior portion of the insula in the left hemisphere. Tract-tracing studies in monkeys demonstrate that the ventral anterior insula has robust bidirectional connections with the ACC (Pandya et al. 1981; Mesulam and Mufson 1982a, 1982b; Vogt and Pandya 1987). These anatomical connections are also evident in correlated activity in the regions, observed in studies of resting-state functional connectivity in monkeys (Hutchison et al. 2011, 2012) and humans (Taylor et al. 2009). This connectivity is a core component of the interoceptive-allostatic network in monkeys (Touroutoglou et al. 2016) and humans (Seeley et al. 2007; Touroutoglou et al. 2012; Kleckner et al. 2017), which subserve many psychological functions including affective experience, memory, and decision-making that jointly rely on allostasis, or continual predictive regulation of the body's internal milieu (Sterling 2012).

As a field, we know relatively little about insula plasticity compared with what is known about amygdala plasticity, and very little about plasticity it its anterior portion that would lead to expansion (rather than atrophy). Studies of neuropathic pain shed some light on insula plasticity and demonstrate variable changes in insula structure across subregions (see Wang et al. 2021 for a review). In patients with trigeminal neuropathic pain, compared with participants without pain, gray matter volume was reduced in the anterior insula, but increased in the posterior insula (Gustin et al. 2011). Meta-analyses of structural neuroimaging studies have also shown that across many different neuropsychiatric disorders (Goodkind et al. 2015) and at the intersection between cognitive impairment and neuropsychiatric disorders (Zacková et al. 2021), changes to insula, ACC and amygdala volumes are the most consistent and robust compared with other brain regions, although such changes were decreases rather than increases in volume, accenting the translational importance of understanding how these regions adapt and reorganize across contexts. Changes to insula volume have also been assessed in the context of auditory deprivation during development (Allen et al. 2008). Congenitally deaf people had significantly greater volumes in the posterior insular lobule, which may be due to greater dependence on visual and motor representations of speech (relative to auditory ones) in these people (Allen et al. 2008). We might then hypothesize that sensory deprivation across other domains, including the putative deprivation of autonomic signals that would result from damage to the ACC, might also increase insula volumes in relevant subregions. Although posterior insula appears to be primarily involved in somatosensory, visual, and motor functions, anterior insula—where we saw changes—is more involved in autonomic and visceral functions (Augustine 1985, 1996; Mesulam and Mufson 1985; Rolls 2016; Evrard 2019), consistent with this deprivation-based hypothesis. Changes to volume in this region could also be driven by an increase in the number of glial cells present as a result of anterograde and retrograde degeneration of axons following damage. Given that the animals investigated here were sacrificed nearly 4 years after lesion surgeries occurred, active inflammation in probably an unlikely cause of our observed differences, but future studies assessing the densities of various cell types in this region will be necessary to determine whether this is the case.

Plasticity in the adult primate brain

Our results demonstrate neural plasticity at the level of subregion volumes in adult primate brains following damage to the ACC. Several different mechanisms could account for the volumetric changes that we observed. Volumetric increases could be due to changes to existing amygdala and insula neurons, including increases in the volume of these neurons, or the complexity of their dendritic arbors (see Anderson 2011 for a discussion of the relationship between cellular and synaptic changes and volumetric changes; see Lamprecht and LeDoux 2004; Caroni et al. 2012 for discussions of plasticity mechanisms more generally). Increases in dendritic arborization and the formation of new synapses have long been established as critical mechanisms, which facilitate recovery of function following brain damage (Keller et al. 1990; Dancause 2005; Dancause and Nudo 2011; Kolb and Teskey 2012). Thus, although we cannot speak to whether the changes that we observed are adaptive, it is a reasonable hypothesis that volumetric increases may have occurred to promote functional recovery after damage. Volumetric changes could also be driven by non-neuronal cell populations, including, but not limited to, glial cells (see Yirmiya and Goshen 2011; Burda and Sofroniew 2014; Sandvig et al. 2018 for reviews). Gliosis is one possible non-compensatory process, and scarring, or edema are others that could contribute to volumetric changes. In our volumetric characterization of both the amygdala and the insula, cytoarchitectural features were used to identify the boundaries between regions. Abnormalities in cytoarchitecture like obvious gliosis or scarring were not noted throughout the course of these comprehensive evaluations. This said, future studies will investigate the numbers, densities, and sizes of both neuronal and non-neuronal cell types towards an understanding of the precise mechanisms that interoceptive-allostatic hubs employ following damage; establishing the observed volumetric increases following ACC damage sets the stage for such future investigations.

A second potential explanation of our findings is that there were changes in the absolute numbers of cells in the lateral nucleus of the amygdala and ventral anterior insula. Whether or not the adult primate brain is capable of neurogenesis has been the subject of debate for decades. There is concrete—and largely uncontested—evidence of adult neurogenesis in the mammalian olfactory bulb and dentate gyrus (e.g. Rakic 1998; Gage 2000; Kornack and Rakic 2001), but the extent to which neurogenesis occurs elsewhere in the brain is somewhat unclear. It was long held that adult neurogenesis occurred very limitedly, if at all (see Rakic 1985 for a review), but there are a number of more recent claims of widespread and significant adult neurogenesis throughout the brain (e.g. Shankle et al. 1998; Gould et al. 1999), which themselves have been called into question (see Rakic 2002 for a discussion) on the basis of failures to replicate and a variety of methodological limitations (see Duque and Spector 2019; Duque et al. 2022 for reviews). Furthermore, while data collected in rodent models have been leveraged as evidence for adult mammalian neurogenesis (e.g. Lindqvist et al. 2006; Stangl and Thuret 2009), the appropriateness of rodent models of neurogenesis for addressing questions regarding primate brain capacity is unclear (see Duque et al. 2022; Hao and Liu 2022 for discussions). The prevailing view is that de novo generation of neurons in the adult brain occurs in a very limited fashion in healthy adult brains.

Although the birth of new neurons may be rare, there is convincing evidence that both maturation of immature neurons and migration of existing neural precursors occurs following major insult to the central nervous system. In monkeys, experimental global cerebral ischemia enhances the proliferation of neural progenitors in the subventricular zone at both the inferior horn (Tonchev et al. 2003) and anterior horn (Tonchev et al. 2005), indicating that damage to the brain is capable of activating endogenous neuronal precursors in multiple regions known to have neurogenic potential. This activation is likely to subserve recovery of function in some regard after the loss of large populations of neurons. And, as previously discussed, damage to the hippocampus in adult monkeys leads to the differentiation of immature neurons (and potential migration of new neurons; Chareyron et al. 2016). Similar processes appear to be at play in humans. Stroke patients exhibit populations of cells expressing markers consistent with newborn neurons localized to cortical infarcts (Jin et al. 2006). The human amygdala, like the monkey amygdala, also appears to have a pool of excitatory neurons which are maintained in an immature state for, potentially, decades, in the paralaminar nucleus which may promote plasticity via maturation later in life (Sorrells et al. 2019). Together, these findings suggest that it is possible, even probable, that damage to the adult brain initiates mechanisms of neuronal differentiation and/or neurogenesis. Further research is needed to determine if our findings can be explained by such mechanisms.

Neuroimaging cannot replace careful histological evaluations

On initial impression, one might imagine that our findings of volumetric expansion in 2 brain regions could have been revealed via analyses of neuroimaging data, which are widely used to compute the volumes of brain regions. The advent of MRI has revolutionized how scientists and clinicians alike can see and evaluate living brains, and such technology is increasingly being used to assess in vivo changes to the brain following insult (particularly in human patients recovering from stroke or resections of brain regions for the treatment of other neurological maladies, e.g. Cramer et al. 2001; Jiang et al. 2010; Yasuda et al. 2010). Despite this increasing use of MRI, there are a number of methodological reasons why such imaging techniques do not currently—and likely will not be able to for the foreseeable future—replicate careful histological analyses, although they may have great utility when employed alongside or when used to motivate careful histological evaluation, particularly if carried out in a longitudinal fashion.

First, MRI is inherently limited by lower resolution, which obscures cytoarchitectonic boundaries and diminishes the ability to accurately characterize small substructures, like amygdala nuclei. Even on ultra-high resolution MR images, the best segmentations of amygdala nuclei are necessarily less detailed than histological segmentations (Entis et al. 2012). In vivo parcellation methods do not allow for automated segmentation at the level of individual amygdala nuclei as can be done on histology (Saygin et al. 2011; Tyszka and Pauli 2016), requiring that nuclei be grouped together into several larger clusters (e.g. Solano-Castiella et al. 2011; Entis et al. 2012) even when diffusion weighted imaging data are available (e.g. Saygin et al. 2011). Furthermore, amygdala nuclei, even in comparison with subfields of the adjacent hippocampus, exhibited lower numerical and spatial reliability when automated segmentations were employed in FreeSurfer 7 (Kahhale et al. 2020), suggesting that caution must be applied even when employing some of the most commonly used techniques for automated segmentation of cortical and subcortical structures. This is perhaps unsurprising given that even protocols for hand-drawing regions-of-interest in the amygdala exhibit heterogeneity (e.g. variation across "expert" raters in the identification of the dorsal extent of the caudal amygdala as discussed by Entis et al. 2012). These challenges reduce confidence in the ability to detect subtle changes to amygdala structure on MRI and make clear the advantage of computing volumes from histology, where clear boundaries are readily identifiable and have long been established across species (Freese and Amaral 2009; Chareyron et al. 2011); even the best MR images cannot provide the specificity we report here.

Characterization of insula structure using MRI presents its own set of challenges. Narrow separation between the putamen, claustrum, and insula introduces difficulties in automated detection of the gray/white matter boundaries intervening these structures (Han et al. 2006). When multiple MRI processing pipelines were compared, insula and para-limbic areas showed the weakest correlations in cortical thickness estimates across pipelines and the lowest estimate reliability (Kharabian Masouleh et al. 2020), suggesting that the application of such automated methods in the insula may result in findings that should be interpreted with caution. An additional study directly comparing in vivo MRI cortical thickness and histologically obtained measures found that MRI quantification consistently overestimated cortical thickness in the insula relative to histological values (Scholtens et al. 2015). In some cases, gross morphology (e.g. the presence of the central insular sulcus) has been used to segment the human insula to obtain subregion volumes from MRIs (e.g. Takahashi et al. 2009). These boundaries are not necessarily directly related to cytoarchitectonic or functional boundaries, which draws the utility of such practice into question. Furthermore, the macaque insula is nearly entirely lissencephalic (Evrard et al. 2014) and so gyral boundaries cannot be used to segment the monkey insula as can be done with the human insula. Finally, although differences in myeloarchitecture across portions of the insula suggest that these values may provide a reliable schema for parcellation of the insula into anatomical subregions on the basis of MRI data (Glasser et al. 2014), further research is needed to determine whether this is possible, produces consistent results, and the extent to which such segmentations map to histological analyses. Even if such segmentation procedures are able to accurately identify gross regions (e.g. granular, dysgranular, and agranular insula), they are unlikely to be able to make the fine-grained distinctions between subregions that we were able to make in this report using histological evidence.

Limitations and future directions

Like all nonhuman primate studies, the interpretation of our findings is inherently constrained by the small sample size, which is notably larger than many histological studies of the monkey brain. Although the sample size for our study is normal (or relatively large, even) for a behavioral neuroscience experiment assessing the impacts of large neurotoxic lesions, it is small for a between groups comparison of multiple brain regions. It is for this reason that we chose to interpret outcomes for which the statistical analyses did not reach the conventional level of significance ($P < 0.05$). Replication of the present experiments is rendered unlikely by the costly (in terms of both research costs and nonhuman primate lives) nature of these kinds of experiments. However, even in the absence of replication, there are avenues for increasing confidence in the changes that we report here. The use of neurotoxic lesions of focal brain regions in the macaque brain is a gold standard for generating causal knowledge about primate brain function (see Murray and Baxter 2006; Vaidya et al. 2019 for reviews). Given the widespread nature of these kinds of

studies, even in the absence of replication of ACC lesions, we can leverage the tissue obtained from other lesion studies assessing nodes in the same network to determine whether they produce convergent findings. That is, we can carry out similar studies assessing, for example, changes to the ACC and insula following selective lesions of the amygdala. Some evidence already exists from similar investigations of other hubs in this network, which lends support to the present findings. Although not necessarily directly comparable to the outcomes we report here due to the use of neonatal rather than adult lesions, Grayson et al. (2017) found expansion of the cingulate cortex following damage to the amygdala, which provides precedence for hypertrophy in this network after damage. Prior studies have assessed the behavioral impacts of adult amygdala lesions (e.g. Emery et al. 2001; Mason et al. 2006; Charbonneau et al. 2021) and orbitofrontal cortex lesions (e.g. Rudebeck and Murray 2008; Babineau et al. 2011), both of which regions exhibit robust connectivity with the regions that we focus on here. Although to our knowledge no prior investigations have assessed the impacts of adult (or neonatal) lesions of the insula in monkeys, such experiments are likely to also yield important insights about the function of this structure and how this network leverages neuroplasticity.

Conclusions

Evaluating the ways in which specific neural networks respond to damage to their constituent hubs is critical for understanding healthy functioning in these networks and harnessing their plastic potential to intervene in people who experience brain damage. Our results provide evidence that damage to interoceptive-allostatic neural hubs can drive plasticity throughout this network—here, in the form of hypertrophy. Strokes impacting the anterior and middle cerebral arteries often impact the ACC and insula, respectively, (Kang and Kim 2008; Raghu et al. 2019) and even in the case of so-called "minor strokes," patients frequently have lasting deficiencies in affective processing once initial sensorimotor impairments have been recovered (Carlsson et al. 2004; Fischer et al. 2010; Hewlett et al. 2014). Our findings provide a foundational understanding of how the interoceptive-allostatic network responds to damage. Beyond focal damage, such as that which occurs in stroke, variable structural changes in this network are likely to subserve deficits in affective processing observed in Alzheimer's disease (García-Cordero et al. 2016; Chaudhary et al. 2022) and neuropsychiatric patients (Khalsa et al. 2018). Emerging evidence also indicates that regions belonging to this network are among those most significantly impacted by SARS-CoV-2 infection (Douaud et al. 2022). Our findings can thus be leveraged in future studies assessing the precise mechanisms through which the interoceptive-allostatic network reorganizes in order to aid in intervention across the myriad conditions that cause degeneration of this network.

Supplementary material

Supplementary material is available at *Cerebral Cortex* online.

Funding

This work was supported by the National Institutes of Health (grants R01MH75702 and P51OD011107, as well as F32MH087067 to EBM). JAC was supported by T32MH082174 and F31AG077797.

Conflict of interest statement: The authors declare no competing financial interests or potential conflicts of interest.

References

Abbott LF, Nelson SB. Synaptic plasticity: taming the beast. *Nat Neurosci*. 2000:3(S11):1178–1183.

Akert K, Orth OS, Harlow HF, Schiltz KA. Learned behavior of rhesus monkeys following neonatal bilateral prefrontal lobotomy. *Science*. 1960:132(3444):1944–1945.

Allen JS, Emmorey K, Bruss J, Damasio H. Morphology of the insula in relation to hearing status and sign language experience. *J Neurosci*. 2008:28(46):11900–11905.

Amaral DG, Insausti R. Retrograde transport of D-[3H]-aspartate injected into the monkey amygdaloid complex. *Exp Brain Res*. 1992:88(2):375–388.

Amaral DG, Price JL. Amygdalo-cortical projections in the monkey (Macaca fascicularis). *J Comp Neurol*. 1984:230(4):465–496.

Anderson BJ. Plasticity of gray matter volume: the cellular and synaptic plasticity that underlies volumetric change. *Dev Psychobiol*. 2011:53(5):456–465.

Armio R-L, Laurikainen H, Ilonen T, Walta M, Salokangas RKR, Koutsouleris N, Hietala J, Tuominen L. Amygdala subnucleus volumes in psychosis high-risk state and first-episode psychosis. *Schizophr Res*. 2020:215:284–292.

Augustine JR. The insular lobe in primates including humans. *Neurol Res*. 1985:7(1):2–10.

Augustine R. Circuitry and fimctional aspects of the insular lobe in primates including humans. *Brain Res Rev*. 1996:22(3):229–244.

Avino TA, Barger N, Vargas MV, Carlson EL, Amaral DG, Bauman MD, Schumann CM. Neuron numbers increase in the human amygdala from birth to adulthood, but not in autism. *Proc Natl Acad Sci U S A*. 2018:115(14):3710–3715.

Babineau BA, Bliss-Moreau E, Machado CJ, Toscano JE, Mason WA, Amaral DG. Context–specific social behavior is altered by orbitofrontal cortex lesions in adult rhesus macaques. *Neuroscience*. 2011:179:80–93.

Bachevalier J, Machado CJ, Kazama A. Behavioral outcomes of late-onset or early-onset orbital frontal cortex (areas 11/13) lesions in rhesus monkeys: orbital frontal lesions alter behavioral adaptation. *Ann N Y Acad Sci*. 2011:1239(1):71–86.

Banta Lavenex P, Amaral DG, Lavenex P. Hippocampal lesion prevents spatial relational learning in adult macaque monkeys. *J Neurosci*. 2006:26(17):4546–4558.

Baroncelli L, Lunghi C. Neuroplasticity of the visual cortex: in sickness and in health. *Exp Neurol*. 2021:335:113515.

Barrett LF, Satpute AB. Large-scale brain networks in affective and social neuroscience: towards an integrative functional architecture of the brain. *Curr Opin Neurobiol*. 2013:23(3):361–372.

Barth C, Nerland S, de Lange A-MG, Wortinger LA, Hilland E, Andreassen OA, Jørgensen KN, Agartz I. In vivo amygdala nuclei volumes in schizophrenia and bipolar disorders. *Schizophr Bull*. 2021:47(5):1431–1441.

Bateman JR, Kawas MI, Craft S, Lockhart SN, Kim J, Sai KKS, Lindquist KA, Whitlow CT. Difference in allostatic interoceptive network connectivity by cognitive status. *Alzheimers Dement*. 2021:17(S6).

Bates D, Maechler M, Bolker B, Walker S. Fitting linear mixed-effects models using lme4. *J Stat Softw*. 2015:67(1):1–48.

Beck H, Yaari Y. Plasticity of intrinsic neuronal properties in CNS disorders. *Nat Rev Neurosci*. 2008:9(5):357–369.

Behrman AL, Bowden MG, Nair PM. Neuroplasticity after spinal cord injury and training: an emerging paradigm shift in rehabilitation and walking recovery. *Phys Ther*. 2006:86(10):1406–1425.

Bernier PJ, Bédard A, Vinet J, Lévesque M, Parent A. Newly generated neurons in the amygdala and adjoining cortex of adult primates. *Proc Natl Acad Sci U S A*. 2002:99(17):11464–11469.

Birba A, Santamaría-García H, Prado P, Cruzat J, Ballesteros AS, Legaz A, Fittipaldi S, Duran-Aniotz C, Slachevsky A, Santibañez R et al. Allostatic-interoceptive overload in frontotemporal dementia. *Biol Psychiatry*. 2022:92(1):54–67.

Bliss-Moreau E, Bauman MD, Amaral DG. Neonatal amygdala lesions result in globally blunted affect in adult rhesus macaques. *Behav Neurosci*. 2011:125(6):848–858.

Bliss-Moreau E, Moadab G, Bauman MD, Amaral DG. The impact of early amygdala damage on juvenile Rhesus macaque social behavior. *J Cogn Neurosci*. 2013:25(12):2124–2140.

Bliss-Moreau E, Moadab G, Santistevan A, Amaral DG. The effects of neonatal amygdala or hippocampus lesions on adult social behavior. *Behav Brain Res*. 2017:322(Pt A):123–137.

Bliss-Moreau E, Santistevan AC, Bennett J, Moadab G, Amaral DG. Anterior cingulate cortex ablation disrupts affective vigor and vigilance. *J Neurosci*. 2021:41(38):8075–8087.

Bonaz B, Lane RD, Oshinsky ML, Kenny PJ, Sinha R, Mayer EA, Critchley HD. Diseases, disorders, and comorbidities of interoception. *Trends Neurosci*. 2021:44(1):39–51.

Burda JE, Sofroniew MV. Reactive gliosis and the multicellular response to CNS damage and disease. *Neuron*. 2014:81(2):229–248.

Burke SN, Barnes CA. Neural plasticity in the ageing brain. *Nat Rev Neurosci*. 2006:7(1):30–40.

Carlsson G, Möller A, Blomstrand C. A qualitative study of the consequences of "hidden dysfunctions" one year after a mild stroke in persons <75 years. *Disabil Rehabil*. 2004:26(23):1373–1380.

Carmichael ST, Price JL. Architectonic subdivision of the orbital and medial prefrontal cortex in the macaque monkey. *J Comp Neurol*. 1994:346(3):366–402.

Caroni P, Donato F, Muller D. Structural plasticity upon learning: regulation and functions. *Nat Rev Neurosci*. 2012:13(7):478–490.

Charbonneau JA, Bennett JL, Bliss-Moreau E. Amygdala or hippocampus damage only minimally impacts affective responding to threat. *Behav Neurosci*. 2021:136(1):30–45.

Charbonneau JA, Maister L, Tsakiris M, Bliss-Moreau E. Rhesus monkeys have an interoceptive sense of their beating hearts. *Proc Natl Acad Sci*. 2022:119(16):e2119868119.

Chareyron LJ, Banta Lavenex P, Amaral DG, Lavenex P. Stereological analysis of the rat and monkey amygdala. *J Comp Neurol*. 2011:519(16):3218–3239.

Chareyron LJ, Amaral DG, Lavenex P. Selective lesion of the hippocampus increases the differentiation of immature neurons in the monkey amygdala. *Proc Natl Acad Sci U S A*. 2016:113(50):14420–14425.

Chaudhary S, Zhornitsky S, Chao HH, van Dyck CH, Li C-SR. Emotion processing dysfunction in alzheimer's disease: an overview of behavioral findings, systems neural correlates, and underlying neural biology. *Am J Alzheimers Dis Other Dement*. 2022:37:153331752210828.

Chen WG, Schloesser D, Arensdorf AM, Simmons JM, Cui C, Valentino R, Gnadt JW, Nielsen L, Hillaire-Clarke CST, Spruance V et al. The emerging science of interoception: sensing, integrating, interpreting, and regulating signals within the self. *Trends Neurosci*. 2021:44(1):3–16.

Craig AD. How do you feel? Interoception: the sense of the physiological condition of the body. *Nat Rev Neurosci*. 2002:3(8):655–666.

Craig AD. (Bud).Interoception: the sense of the physiological condition of the body. *Curr Opin Neurobiol*. 2003:13(4):500–505.

Craig AD. (Bud).How do you feel — now? The anterior insula and human awareness. *Nat Rev Neurosci*. 2009:10(1):59–70.

Cramer SC, Nelles G, Schaechter JD, Kaplan JD, Finklestein SP, Rosen BR. A functional MRI study of three motor tasks in the evaluation of stroke recovery. *Neurorehabil Neural Repair*. 2001:15(1):1–8.

Crossley NA, Mechelli A, Scott J, Carletti F, Fox PT, McGuire P, Bullmore ET. The hubs of the human connectome are generally implicated in the anatomy of brain disorders. *Brain*. 2014:137(8):2382–2395.

Croxson PL, Browning PGF, Gaffan D, Baxter MG. Acetylcholine facilitates recovery of episodic memory after brain damage. *J Neurosci*. 2012:32(40):13787–13795.

Dancause N. Extensive cortical rewiring after brain injury. *J Neurosci*. 2005:25(44):10167–10179.

Dancause N, Nudo RJ. Shaping plasticity to enhance recovery after injury. In: *Progress in brain research*. Oxford, UK: Elsevier; 2011. pp. 273–295

Darling WG, Ge J, Stilwell-Morecraft KS, Rotella DL, Pizzimenti MA, Morecraft RJ. Hand motor recovery following extensive frontoparietal cortical injury is accompanied by upregulated corticoreticular projections in monkey. *J Neurosci*. 2018:38(28):6323–6339.

De Giglio L, Tommasin S, Petsas N, Patrizia P. The role of fMRI in the assessment of neuroplasticity in MS: a systematic review. *Neural Plast*. 2018:2018:1–27.

deCampo DM, Fudge JL. Where and what is the paralaminar nucleus? A review on a unique and frequently overlooked area of the primate amygdala. *Neurosci Biobehav Rev*. 2012:36(1):520–535.

Dimyan MA, Cohen LG. Neuroplasticity in the context of motor rehabilitation after stroke. *Nat Rev Neurol*. 2011:7(2):76–85.

Douaud G, Lee S, Alfaro-Almagro F, Arthofer C, Wang C, McCarthy P, Lange F, Andersson JLR, Griffanti L, Duff E et al. SARS-CoV-2 is associated with changes in brain structure in UK biobank. *Nature*. 2022:604(7907):697–707.

Dum R, Strick P. Motor areas in the frontal lobe of the primate. *Physiol Behav*. 2002:77(4–5):677–682.

Duque A, Spector R. A balanced evaluation of the evidence for adult neurogenesis in humans: implication for neuropsychiatric disorders. *Brain Struct Funct*. 2019:224(7):2281–2295.

Duque A, Arellano JI, Rakic P. An assessment of the existence of adult neurogenesis in humans and value of its rodent models for neuropsychiatric diseases. *Mol Psychiatry*. 2022:27(1):377–382.

Emery NJ, Capitanio JP, Mason WA, Machado CJ, Mendoza SP. The effects of bilateral lesions of the amygdala on dyadic social interactions in rhesus monkeys (Macaca Mulatta). *Behav Neurosci*. 2001:115(3):515–544.

Entis JJ, Doerga P, Barrett LF, Dickerson BC. A reliable protocol for the manual segmentation of the human amygdala and its subregions using ultra-high resolution MRI. *NeuroImage*. 2012:60(2):1226–1235.

Evrard HC. The organization of the primate insular cortex. *Front Neuroanat*. 2019:13:21.

Evrard HC, Logothetis NK, Bud Craig AD. Modular architectonic organization of the insula in the macaque monkey: architectonic organization of macaque insula. *J Comp Neurol*. 2014:522(1):64–97.

Fischer U, Baumgartner A, Arnold M, Nedeltchev K, Gralla J, Marco De Marchis G, Kappeler L, Mono M-L, Brekenfeld C, Schroth G et al. What is a minor stroke? *Stroke*. 2010:41(4):661–666.

Fornito A, Zalesky A, Breakspear M. The connectomics of brain disorders. *Nat Rev Neurosci*. 2015:16(3):159–172.

Fossati P, Radtchenko A, Boyer P. Neuroplasticity: from MRI to depressive symptoms. *Eur Neuropsychopharmacol*. 2004:14:S503–S510.

Freese JL, Amaral DG. Neuroanatomy of the primate amygdala. In: Whalen PJ, Phelps EA, editors. *The human amygdala*. New York, NY, USA: The Guilford Press; 2009. pp. 3–42

Froudist-Walsh S, Browning PG, Young JJ, Murphy KL, Mars RB, Fleysher L, Croxson PL. Macro-connectomics and microstructure

predict dynamic plasticity patterns in the non-human primate brain. *Elife*. 2018:7:e34354.

Fudge JL, deCampo DM, Becoats KT. Revisiting the hippocampal–amygdala pathway in primates: association with immature-appearing neurons. *Neuroscience*. 2012:212:104–119.

Gage FH. Mammalian neural stem cells. *Science*. 2000:287(5457): 1433–1438.

García-Cordero I, Sedeño L, de la Fuente L, Slachevsky A, Forno G, Klein F, Lillo P, Ferrari J, Rodriguez C, Bustin J et al. Feeling, learning from and being aware of inner states: interoceptive dimensions in neurodegeneration and stroke. *Philos Trans R Soc B*. 2016:371(1708):20160006.

Glasser MF, Goyal MS, Preuss TM, Raichle ME, Van Essen DC. Trends and properties of human cerebral cortex: correlations with cortical myelin content. *NeuroImage*. 2014:93:165–175.

Gomis-Rüth S, Wierenga CJ, Bradke F. Plasticity of polarization: changing dendrites into axons in neurons integrated in neuronal circuits. *Curr Biol*. 2008:18(13):992–1000.

Goodkind M, Eickhoff SB, Oathes DJ, Jiang Y, Chang A, Jones-Hagata LB, Ortega BN, Zaiko YV, Roach EL, Korgaonkar MS et al. Identification of a common neurobiological substrate for mental illness. *JAMA Psychiat*. 2015:72(4):305–315.

Gould E, Reeves AJ, Graziano MSA, Gross CG. Neurogenesis in the neocortex of adult Primates. *Science*. 1999:286(5439):548–552.

Grayson DS, Bliss-Moreau E, Bennett J, Lavenex P, Amaral DG. Neural reorganization due to neonatal amygdala lesions in the rhesus monkey: changes in morphology and network structure. *Cereb Cortex*. 2017:27(6):3240–3253.

Gulyaeva NV. Molecular mechanisms of neuroplasticity: an expanding universe. *Biochemistry (Mosc)*. 2017:82(3):237–242.

Gundersen HJG, Jensen EB. The efficiency of systematic sampling in stereology and its prediction. *J Microsc*. 1987:147(3):229–263.

Gustin SM, Peck CC, Wilcox SL, Nash PG, Murray GM, Henderson LA. Different pain, different brain: thalamic anatomy in neuropathic and non-neuropathic chronic pain syndromes. *J Neurosci*. 2011:31(16):5956–5964.

Han X, Jovicich J, Salat D, van der Kouwe A, Quinn B, Czanner S, Busa E, Pacheco J, Albert M, Killiany R et al. Reliability of MRI-derived measurements of human cerebral cortical thickness: the effects of field strength, scanner upgrade and manufacturer. *NeuroImage*. 2006:32(1):180–194.

Hao Z-Z, Liu S. Robust adult neurogenesis in the primate hippocampus. *Nat Neurosci*. 2022:25:684–685.

Hermann DM, Chopp M. Promoting brain remodelling and plasticity for stroke recovery: therapeutic promise and potential pitfalls of clinical translation. *The Lancet Neurology*. 2012:11(4):369–380.

Hewlett KA, Kelly MH, Corbett D. 'Not-so-minor' stroke: lasting psychosocial consequences of anterior cingulate cortical ischemia in the rat. *Exp Neurol*. 2014:261:543–550.

Hübener M, Bonhoeffer T. Neuronal plasticity: beyond the critical period. *Cell*. 2014:159(4):727–737.

Hutchison RM, Leung LS, Mirsattari SM, Gati JS, Menon RS, Everling S. Resting-state networks in the macaque at 7T. *NeuroImage*. 2011:56(3):1546–1555.

Hutchison RM, Womelsdorf T, Gati JS, Leung LS, Menon RS, Everling S. Resting-state connectivity identifies distinct functional networks in macaque cingulate cortex. *Cereb Cortex*. 2012:22(6): 1294–1308.

Ismail FY, Fatemi A, Johnston MV. Cerebral plasticity: windows of opportunity in the developing brain. *Eur J Paediatr Neurol*. 2017:21(1):23–48.

Jellinger KA, Attems J. Neuropathological approaches to cerebral aging and neuroplasticity. *Dialogues Clin Neurosci*. 2013:15(1): 29–43.

Jiang Q, Zhang ZG, Chopp M. MRI of stroke recovery. *Stroke*. 2010:41(2):410–414.

Jin K, Wang X, Xie L, Mao XO, Zhu W, Wang Y, Shen J, Mao Y, Banwait S, Greenberg DA. Evidence for stroke-induced neurogenesis in the human brain. *Proc Natl Acad Sci U S A*. 2006:103(35):13198–13202.

Joshi SH, Espinoza RT, Pirnia T, Shi J, Wang Y, Ayers B, Leaver A, Woods RP, Narr KL. Structural plasticity of the hippocampus and amygdala induced by electroconvulsive therapy in major depression. *Biol Psychiatry*. 2016:79(4):282–292.

Kahhale I, Buser NJ, Madan CR, Hanson JL. Quantifying numerical and spatial reliability of amygdala and hippocampal subdivisions in freesurfer (preprint). *Neuroscience*. 2020.

Kang SY, Kim JS. Anterior cerebral artery infarction: stroke mechanism and clinical-imaging study in 100 patients. *Neurology*. 2008:70(Issue 24, Part 2):2386–2393.

Kazama AM, Heuer E, Davis M, Bachevalier J. Effects of neonatal amygdala lesions on fear learning, conditioned inhibition, and extinction in adult macaques. *Behav Neurosci*. 2012:126(3): 392–403.

Keller A, Arissian K, Asanuma H. Formation of new synapses in the cat motor cortex following lesions of the deep cerebellar nuclei. *Exp Brain Res*. 1990:80(1):23–33.

Kennard MK. Age and other factors in motor recovery from precentral lesions in monkeys. *Am J Phys*. 1936:115(1):138–146.

Kennard MA. Cortical reorganization of motor function: studies on series of monkeys of various ages from infancy to maturity. *Arch NeurPsych*. 1942:48(2):227.

Khalsa SS, Adolphs R, Cameron OG, Critchley HD, Davenport PW, Feinstein JS, Feusner JD, Garfinkel SN, Lane RD, Mehling WE et al. Interoception and mental health: a roadmap. *Biol Psychiatry*. 2018:3(6):501–513.

Kharabian Masouleh S, Eickhoff SB, Zeighami Y, Lewis LB, Dahnke R, Gaser C, Chouinard-Decorte F, Lepage C, Scholtens LH, Hoffstaedter F et al. Influence of processing pipeline on cortical thickness measurement. *Cereb Cortex*. 2020:30(9):5014–5027.

Kleckner IR, Zhang J, Touroutoglou A, Chanes L, Xia C, Simmons WK, Quigley KS, Dickerson BC, Feldman BL. Evidence for a large-scale brain system supporting allostasis and interoception in humans. *Nat Hum Behav*. 2017:1(5):0069.

Kolb B. Brain development, plasticity, and behavior. *Am Psychol*. 1989:44(9):1203–1212.

Kolb B, Gibb R. Brain plasticity and recovery from early cortical injury. *Dev Psychobiol*. 2007:49(2):107–118.

Kolb B, Gibb R. Principles of neuroplasticity and behavior. In: Stuss DT, Winocur G, Robertson IH, editors. *Cognitve neurorehabilitation: evidence and application*. 2nd ed. Cambridge University Press; 2010

Kolb B, Gibb R. Searching for the principles of brain plasticity and behavior. *Cortex*. 2014:58:251–260.

Kolb B, Teskey GC. Age, experience, injury, and the changing brain. *Dev Psychobiol*. 2012:54(3):311–325.

Kolb B, Harker A, Gibb R. Principles of plasticity in the developing brain. *Dev Med Child Neurol*. 2017:59(12):1218–1223.

Kornack DR, Rakic P. The generation, migration, and differentiation of olfactory neurons in the adult primate brain. *Proc Natl Acad Sci U S A*. 2001:98(8):4752–4757.

Kraus C, Ganger S, Losak J, Hahn A, Savli M, Kranz GS, Baldinger P, Windischberger C, Kasper S, Lanzenberger R. Gray matter and intrinsic network changes in the posterior cingulate cortex after selective serotonin reuptake inhibitor intake. *NeuroImage*. 2014:84:236–244.

Krockenberger M, Saleh TO, Logothetis NK, Evrard HC. Connection "stripes" in the primate insula (preprint). *Neuroscience*. 2020.

Lamprecht R, LeDoux J. Structural plasticity and memory. *Nat Rev Neurosci*. 2004:5(1):45–54.

Lavenex P, Lavenex PB. Spatial relational memory in 9-month-old macaque monkeys. *Learn Mem*. 2006:13(1):84–96.

Lavenex P, Lavenex PB, Bennett JL, Amaral DG. Postmortem changes in the neuroanatomical characteristics of the primate brain: hippocampal formation. *J Comp Neurol*. 2009:512(1): 27–51.

Lenth RV. Emmeans: estimated marginal means, aka least-squares means. 2021.

Lindqvist A, Mohapel P, Bouter B, Frielingsdorf H, Pizzo D, Brundin P, Erlanson-Albertsson C. High-fat diet impairs hippocampal neurogenesis in male rats. *Eur J Neurol*. 2006:13(12):1385–1388.

Lubrini G, Martín-Montes A, Díez-Ascaso O, Díez-Tejedor E. Brain disease, connectivity, plasticity and cognitive therapy: a neurological view of mental disorders. *Neurología (English Edition)*. 2018:33(3): 187–191.

Lyden H, Espinoza RT, Pirnia T, Clark K, Joshi SH, Leaver AM, Woods RP, Narr KL. Electroconvulsive therapy mediates neuroplasticity of white matter microstructure in major depression. *Transl Psychiatry*. 2014:4(4):e380–e380.

Mason WA, Capitanio JP, Machado CJ, Mendoza SP, Amaral DG. Amygdalectomy and responsiveness to novelty in rhesus monkeys (Macaca mulatta): generality and individual consistency of effects. *Emotion*. 2006:6(1):73–81.

Matus A. Actin-based plasticity in dendritic spines. *Science*. 2000:290(5492):754–758.

McEwen BS, Stellar E. Stress and the individual: mechanisms leading to disease. *Arch Intern Med*. 1993:153(18):2093.

Mesulam M-M, Mufson EJ. Insula of the old world monkey. III: efferent cortical output and comments on function. *J Comp Neurol*. 1982a:212(1):38–52.

Mesulam MM, Mufson EJ. Insula of the old world monkey. Architectonics in the insulo-orbito-temporal component of the paralimbic brain. *J Comp Neurol*. 1982b:212(1):1–22.

Mesulam M-M, Mufson EJ. The insula of Reil in man and monkey. In: Peters A, Jones EG, editors. *Association and auditory cortices. Cerebral cortex*. Boston, MA: Springer US; 1985. pp. 179–226

Moadab G, Bliss-Moreau E, Amaral DG. Adult social behavior with familiar partners following neonatal amygdala or hippocampus damage. *Behav Neurosci*. 2015:129(3):339–350.

Morrison JH, Baxter MG. The ageing cortical synapse: hallmarks and implications for cognitive decline. *Nat Rev Neurosci*. 2012:13(4): 240–250.

Murata Y, Higo N, Hayashi T, Nishimura Y, Sugiyama Y, Oishi T, Tsukada H, Isa T, Onoe H. Temporal plasticity involved in recovery from manual dexterity deficit after motor cortex lesion in macaque monkeys. *J Neurosci*. 2015:35(1):84–95.

Murphy TH, Corbett D. Plasticity during stroke recovery: from synapse to behaviour. *Nat Rev Neurosci*. 2009:10(12):861–872.

Murray EA, Baxter MG. Cognitive neuroscience and nonhuman primates: lesion studies. In: Senior C, Russell T, Gazzaniga MS, editors. *Methods in mind*. Cambridge, MA, USA: MIT Press; 2006. pp. 43–69

O'Leary DDM, Ruff NL, Dyck RH. Development, critical period plasticity, and adult reorganizations of mammalian somatosensory systems. *Curr Opin Neurobiol*. 1994:4(4):535–544.

Ousdal OT, Milde AM, Hafstad GS, Hodneland E, Dyb G, Craven AR, Melinder A, Endestad T, Hugdahl K. The association of PTSD symptom severity with amygdala nuclei volumes in traumatized youths. *Transl Psychiatry*. 2020:10(1):288.

Pandya DN, Van Hoesen GW, Domesick VB. A cingulo-amygdaloid projection in the rhesus monkey. *Brain Res*. 1973:61:369–373.

Pandya DN, Van Hoesen GW, Mesulam MM. Efferent connections of the cingulate gyrus in the rhesus monkey. *Exp Brain Res*. 1981: 42–42(3–4):319–330.

Phillips KA, Bales KL, Capitanio JP, Conley A, Czoty PW, 't Hart BA, Hopkins WD, Hu S-L, Miller LA, Nader MA et al. Why primate models matter. *Am J Primatol*. 2014:76(9):801–827.

Pitkänen A, Kemppainen S. Comparison of the distribution of calcium-binding proteins and intrinsic connectivity in the lateral nucleus of the rat, monkey, and human amygdala. *Pharmacol Biochem Behav*. 2002:71(3):369–377.

Porrino LJ, Crane AM, Goldman-Rakic PS. Direct and indirect pathways from the amygdala to the frontal lobe in rhesus monkeys. *J Comp Neurol*. 1981:198(1):121–136.

Power JD, Schlaggar BL. Neural plasticity across the lifespan. *WIREs Dev Biol*. 2017:6(1):e216.

Price J, Russchen F, Amaral D. The limbic region. II. The amygdaloid complex. In: Bjorkland A, Hokfelt T, Swanson L, editors. *Handbook of chemical neuroanatomy*. Amsterdam: Elsevier; 1987. pp. 279–381

Pritchard TC, Hamilton RB, Norgren R. Projections of the parabrachial nucleus in the old world monkey. *Exp Neurol*. 2000:165(1):101–117.

R Core Team. *R: a language and environment for statistical computing*. Vienna, Austria: R Foundation for Statistical Computing; 2019

Raghu ALB, Parker T, van Wyk A, Green AL. Insula stroke: the weird and the worrisome. *Postgrad Med J*. 2019:95(1127):497–504.

Raichle ME. The brain's default mode network. *Annu Rev Neurosci*. 2015:38(1):433–447.

Rakic P. Limits of neurogenesis in primates. *Science*. 1985:227(4690): 1054–1056.

Rakic P. Young neurons for old brains? *Nat Neurosci*. 1998:1(8): 645–647.

Rakic P. Neurogenesis in adult primate neocortex: an evaluation of the evidence. *Nat Rev Neurosci*. 2002:3(1):65–71.

Reichert JL, Schöpf V. Olfactory loss and regain: lessons for neuroplasticity. *Neuroscientist*. 2018:24(1):22–35.

Reid LB, Boyd RN, Cunnington R, Rose SE. Interpreting intervention induced neuroplasticity with fMRI: the case for multimodal imaging strategies. *Neural Plast*. 2016:2016:1–13.

Robertson IH, Murre JMJ. Rehabilitation of brain damage: brain plasticity and principles of guided recovery. *Psychol Bull*. 1999:125(5): 544–575.

Rolls ET. Functions of the anterior insula in taste, autonomic, and related functions. *Brain Cogn*. 2016:110:4–19.

Rossini PM, Dal Forno G. Neuronal post-stroke plasticity in the adult. *Restor Neurol Neurosci*. 2004:22(3–5):193–206.

Rudebeck PH, Murray EA. Amygdala and orbitofrontal cortex lesions differentially influence choices during object reversal learning. *J Neurosci*. 2008:28(33):8338–8343.

Ryugo D. Auditory neuroplasticity, hearing loss and cochlear implants. *Cell Tissue Res*. 2015:361(1):251–269.

Salm AK, Pavelko M, Krouse EM, Webster W, Kraszpulski M, Birkle DL. Lateral amygdaloid nucleus expansion in adult rats is associated with exposure to prenatal stress. *Dev Brain Res*. 2004:148(2): 159–167.

Sandvig I, Augestad IL, Håberg AK, Sandvig A. Neuroplasticity in stroke recovery. The role of microglia in engaging and modifying synapses and networks. *Eur J Neurosci*. 2018:47(12):1414–1428.

Saygin ZM, Osher DE, Augustinack J, Fischl B, Gabrieli JDE. Connectivity-based segmentation of human amygdala nuclei using probabilistic tractography. *NeuroImage*. 2011:56(3): 1353–1361.

Scholtens LH, de Reus MA, van den Heuvel MP. Linking contemporary high resolution magnetic resonance imaging to the von economo legacy: a study on the comparison of MRI cortical thickness and histological measurements of cortical structure: linking contemporary high resolution MRI to the Von Economo legacy. *Hum Brain Mapp*. 2015:36(8):3038–3046.

Seeley WW, Menon V, Schatzberg AF, Keller J, Glover GH, Kenna H, Reiss AL, Greicius MD. Dissociable intrinsic connectivity networks for salience processing and executive control. *J Neurosci*. 2007:27(9):2349–2356.

Seth AK. Interoceptive inference, emotion, and the embodied self. *Trends Cogn Sci*. 2013:17(11):565–573.

Shankle WR, Landing BH, Rafii MS, Schiano A, Chen JM, Hara J. Evidence for a postnatal doubling of neuron number in the developing human cerebral cortex between 15 months and 6 years. *J Theor Biol*. 1998:191(2):115–140.

Sharma N, Classen J, Cohen LG. Neural plasticity and its contribution to functional recovery. In: *Handbook of clinical neurology*. Oxford, UK: Elsevier; 2013. pp. 3–12

Shipley MT, Sanders MS. Special senses are really special: evidence for a reciprocal, bilateral pathway between insular cortex and nucleus parabrachialis. *Brain Res Bull*. 1982:8(5):493–501.

Sidhu MK, Stretton J, Winston GP, McEvoy AW, Symms M, Thompson PJ, Koepp MJ, Duncan JS. Memory network plasticity after temporal lobe resection: a longitudinal functional imaging study. *Brain*. 2016:139(2):415–430.

Snijders TAB. Power and sample size in multilevel modeling. *Encyclopedia of statistics in behavioral science*. 2005:3:1570–1573.

Solano-Castiella E, Schäfer A, Reimer E, Türke E, Pröger T, Lohmann G, Trampel R, Turner R. Parcellation of human amygdala in vivo using ultra high field structural MRI. *NeuroImage*. 2011:58(3):741–748.

Sorrells SF, Paredes MF, Velmeshev D, Herranz-Pérez V, Sandoval K, Mayer S, Chang EF, Insausti R, Kriegstein AR, Rubenstein JL et al. Immature excitatory neurons develop during adolescence in the human amygdala. *Nat Commun*. 2019:10(1):2748.

Stangl D, Thuret S. Impact of diet on adult hippocampal neurogenesis. *Genes Nutr*. 2009:4(4):271–282.

Stee W, Peigneux P. Post-learning micro- and macro-structural neuroplasticity changes with time and sleep. *Biochem Pharmacol*. 2021:191:114369.

Stefanacci L, Amaral DG. Topographic organization of cortical inputs to the lateral nucleus of the macaque monkey amygdala: a retrograde tracing study. *J Comp Neurol*. 2000:421(1):52–79.

Stefanacci L, Amaral DG. Some observations on cortical inputs to the macaque monkey amygdala: an anterograde tracing study. *J Comp Neurol*. 2002:451(4):301–323.

Sterling P. Allostasis: a model of predictive regulation. *Physiol Behav*. 2012:106(1):5–15.

Straka H, Vibert N, Vidal PP, Moore LE, Dutia MB. Intrinsic membrane properties of vertebrate vestibular neurons: function, development and plasticity. *Prog Neurobiol*. 2005:76(6):349–392.

Takahashi T, Wood SJ, Soulsby B, McGorry PD, Tanino R, Suzuki M, Velakoulis D, Pantelis C. Follow-up MRI study of the insular cortex in first-episode psychosis and chronic schizophrenia. *Schizophr Res*. 2009:108(1–3):49–56.

Taylor KS, Seminowicz DA, Davis KD. Two systems of resting state connectivity between the insula and cingulate cortex. *Hum Brain Mapp*. 2009:30(9):2731–2745.

Tonchev AB, Yamashima T, Zhao L, Okano HJ, Okano H. Proliferation of neural and neuronal progenitors after global brain ischemia in young adult macaque monkeys. *Mol Cell Neurosci*. 2003:23(2):292–301.

Tonchev AB, Yamashima T, Sawamoto K, Okano H. Enhanced proliferation of progenitor cells in the subventricular zone and limited neuronal production in the striatum and neocortex of adult macaque monkeys after global cerebral ischemia. *J Neurosci Res*. 2005:81(6):776–788.

Touroutoglou A, Hollenbeck M, Dickerson BC, Barrett LF. Dissociable large-scale networks anchored in the right anterior insula subserve affective experience and attention. *NeuroImage*. 2012:60(4):1947–1958.

Touroutoglou A, Bliss-Moreau E, Zhang J, Mantini D, Vanduffel W, Dickerson BC, Barrett LF. A ventral salience network in the macaque brain. *NeuroImage*. 2016:132:190–197.

Turkeltaub PE. A taxonomy of brain–behavior relationships after stroke. *J Speech Lang Hear Res*. 2019:62(11):3907–3922.

Turrigiano G. Homeostatic synaptic plasticity: local and global mechanisms for stabilizing neuronal function. *Cold Spring Harb Perspect Biol*. 2012:4(1):a005736–a005736.

Tyszka JM, Pauli WM. In vivo delineation of subdivisions of the human amygdaloid complex in a high-resolution group template: in vivo amygdala subdivisions. *Hum Brain Mapp*. 2016:37(11):3979–3998.

Vaidya AR, Pujara MS, Petrides M, Murray EA, Fellows LK. Lesion studies in contemporary neuroscience. *Trends Cogn Sci*. 2019:23(8):653–671.

Vestergaard-Poulsen P, van Beek M, Skewes J, Bjarkam CR, Stubberup M, Bertelsen J, Roepstorff A. Long-term meditation is associated with increased gray matter density in the brain stem. *Neuroreport*. 2009:20(2):170–174.

Vincent JL, Patel GH, Fox MD, Snyder AZ, Baker JT, Van Essen DC, Zempel JM, Snyder LH, Corbetta M, Raichle ME. Intrinsic functional architecture in the anaesthetized monkey brain. *Nature*. 2007:447(7140):83–86.

Vitureira N, Letellier M, Goda Y. Homeostatic synaptic plasticity: from single synapses to neural circuits. *Curr Opin Neurobiol*. 2012:22(3):516–521.

Vogt BA, editors. *Cingulate neurobiology and disease*. Oxford, UK: Oxford University Press; 2009

Vogt BA, Pandya DN. Cingulate cortex of the rhesus monkey: II. Cortical afferents. *J Comp Neurol*. 1987:262(2):271–289.

Vogt BA, Vogt L, Farber NB, Bush G. Architecture and neurocytology of monkey cingulate gyrus. *J Comp Neurol*. 2005:485(3):218–239.

Wang N, Zhang Y-H, Wang J-Y, Luo F. Current understanding of the involvement of the insular cortex in neuropathic pain: a narrative review. *IJMS*. 2021:22(5):2648.

Yachnis AT, Roper SN, Love A, Fancey JT, Muir D. Bcl-2 immunoreactive cells with immature neuronal phenotype exist in the nonepileptic adult human brain. *J Neuropathol Exp Neurol*. 2000:59(2):113–119.

Yasuda CL, Valise C, Saúde AV, Pereira AR, Pereira FR, Ferreira Costa AL, Morita ME, Betting LE, Castellano G, Mantovani Guerreiro CA et al. Dynamic changes in white and gray matter volume are associated with outcome of surgical treatment in temporal lobe epilepsy. *NeuroImage*. 2010:49(1):71–79.

Yirmiya R, Goshen I. Immune modulation of learning, memory, neural plasticity and neurogenesis. *Brain Behav Immun*. 2011:25(2):181–213.

Yogarajah M, Focke NK, Bonelli SB, Thompson P, Vollmar C, McEvoy AW, Alexander DC, Symms MR, Koepp MJ, Duncan JS. The structural plasticity of white matter networks following anterior temporal lobe resection. *Brain*. 2010:133(8):2348–2364.

Yushkevich PA, Piven J, Hazlett HC, Smith RG, Ho S, Gee JC, Gerig G. User-guided 3D active contour segmentation of anatomical structures: significantly improved efficiency and reliability. *NeuroImage*. 2006:31(3):1116–1128.

Zacková L, Jáni M, Brázdil M, Nikolova YS, Marečková K. Cognitive impairment and depression: meta-analysis of structural magnetic resonance imaging studies. *NeuroImage*. 2021:32:102830.